THE EARLY MIOCENE CAPE BLANCO FLORA OF COASTAL OREGON

by

LISA FRANCIS EMERSON

A DISSERTATION

Presented to the Department of Geological Sciences
and the Graduate School of the University of Oregon
in partial fulfillment of the requirements
for the degree of
Doctor of Philosophy

September 2009

University of Oregon Graduate School

Confirmation of Approval and Acceptance of Dissertation prepared by:

Lisa Emerson

Title:

"The Early Miocene Cape Blanco Flora of coastal Oregon"

This dissertation has been accepted and approved in partial fulfillment of the requirements for the Doctor of Philosophy degree in the Department of Geological Sciences by:

Gregory Retallack, Chairperson, Geological Sciences
Rebecca Dorsey, Member, Geological Sciences
Joshua Roering, Member, Geological Sciences
Barbara Roy, Outside Member, Biology

and Richard Linton, Vice President for Research and Graduate Studies/Dean of the Graduate School for the University of Oregon.

September 5, 2009

Original approval signatures are on file with the Graduate School and the University of Oregon Libraries.

An Abstract of the Dissertation of

Lisa Francis Emerson for the degree of Doctor of Philosophy

in the Department of Geological Sciences to be taken September 2009

Title: THE EARLY MIOCENE CAPE BLANCO FLORA OF COASTAL OREGON

Approved: _____

Gregory J. Retallack

This dissertation establishes the age, depositional environment, composition, and climatic conditions for the Cape Blanco flora. The paleotemperature estimated by the Cape Blanco flora, the Temblor flora of California, and the Seldovia flora of Alaska are then compared with sea surface temperatures estimated from oxygen isotope analysis of benthic foraminifera.

The unconformity-bound shallow marine sandstone of Floras Lake includes a redeposited tuff bed which contains fossil leaves at Cape Blanco. An $^{40}Ar/^{39}Ar$ age of 18.26 ± 0.86 Ma is presented for the tuff as well as a paleomagnetic stratigraphy of the sandstone. Sedimentary structures of the tuff bed are evidence that the tuff was deposited at or just above the strand line. The depth of tuff deposition was shallower than the adjacent marine sands, and this short-lived shoaling may have been a result of increased sediment supply.

The fossil flora was an oak forest with numerous species of Fagaceae. Additional components include lanceolate Salicaceae leaves, entire margined Lauraceae, fragmentary Betulaceae, and lobed Platanaceae. Coniferous debris, charcoal, Equisetales, and Typhaceae forms are also figured. Ten leaf forms could not be confidently assigned to established names but are described, figured, and called angiosperm forms 1-10. In total 44 unique forms are identified. The size and margin type of the dicot specimens are quantified, and by comparison with known modern floras, a former mean annual precipitation of 201 (+86, -61) cm and a former mean annual temperature of 18.26 ± 2.6°C are estimated.

The paleotemperature of the ~17.5 Ma Seldovia Flora and the ~17.5 Ma Temblor Flora are estimated using the same method, establishing a ~0.7°C per degree of latitude temperature gradient for the northern hemisphere temperate zone. The leaf based gradient is steeper than the sea surface temperature gradient, of ~0.26°C per degree of latitude as estimated from oxygen isotopic composition of foraminifera collected from ocean sediment cores. Both fossil leaf and isotope methods suggest that the early Miocene was ~5°C warmer than today.

This thesis includes unpublished co-authored material.

CURRICULUM VITAE

NAME OF AUTHOR: Lisa Francis Emerson

PLACE OF BIRTH: Redmond, Oregon USA

DATE OF BIRTH: October 16, 1979

GRADUATE AND UNDERGRADUATE SCHOOLS ATTENDED:

       University of Oregon, Eugene, OR
       Dartmouth College, Hanover, NH

DEGREES AWARDED:

       Doctor of Philosophy, Geological Sciences, 2009, University of Oregon

       Bachelor of Arts, 2001, Earth Science, Dartmouth College

AREAS OF SPECIAL INTEREST:

       Neogene Stratigraphy
       Paleobotany
       Paleoclimate

PROFESSIONAL EXPERIENCE:

       Graduate Teaching Fellow, University of Oregon Department of Geological
          Sciences, September 2004 to June 2009

       Geoscience Intern, ExxonMobil Exploration Company, Houston, TX, Spring
          2008

       Geoscience Intern, BP North America, Houston, TX, Summer 2007

       Naturalist, Aspen Center for Environmental Studies, Aspen, CO, 2002-2004

GRANTS, AWARDS AND HONORS:

Baldwin Fellowship, University of Oregon Department of Geological Sciences, $1,000.00, June 2009

Dunbar Scholarship, University of Oregon, College of Arts and Sciences, $5,000.00, June 2008

Baldwin Fellowship, University of Oregon Department of Geological Sciences, $1,200.00, June 2007

Condon Fellowship, University of Oregon Department of Geological Sciences, $600.00, June 2006

University of Oregon, Graduate School Research Award to attend the Advances in Paleobotany Conference, January 2006

Baldwin Fellowship, University of Oregon, Department of Geological Sciences, $300.00, June 2005

The Geological Society of America, Student Grant, "Climatic and Biogeographical Implications of the 12 Ma cape Blanco Flora, Cape Blanco, OR, $1,500.00, May 2005

Dartmouth College Earth Science Department, Student Grant, $1,500.00, September 2000

PUBLICATIONS:

Raymond, Kristina R., Prothero, D., Emerson, L., Retallack, G., 2008, Magentostratigraphy of the lower Miocene Sandstone of Floras Lake and the C ape Blanco Flora, Oregon. Geological Society of America abstracts with programs, 40 (6), 477.

Emerson, L. F., and Rempel, A. W., 2007, Thresholds in the sliding resistance of simulated basal ice. The Cryosphere, v. 1, p. 11-19.

Emerson, L. F., and Retallack, G. J., 2007, Miocene coastal vegetation preserved by volcanic eruption at Cape Blanco, OR. Geological Society of America abstracts with programs, 39 (6), 401.

Emerson, L. F., Soule, A., Belien, I., Deardorff, N., Gottesfeld, E., Johnson, E., McKay, D., and Wisely, B. A., 2007, Implementation of ground-based LiDAR, total station, and GPS in an advanced geophysical study of basaltic cinder cone morphology, Four Craters Volcanic Field, Oregon. Geological Society of America abstracts with programs, 39 (6), 123.

Emerson, Lisa F. and Rempel, Alan W., 2006, Laboratory Study of the Frictional Properties of Simulated Basal ice. Eos Trans. AGU, 87 (52) Fall Meeting Suppl., Abstract C31A-1245.

Emerson, Lisa F. and Retallack, Gregory J., 2006, A nearest living relative comparison of the Cape Blanco Flora, Oregon. USA. Advances in paleobotany conference; Gainesville, Florida, USA, March 2006.

Emerson, Lisa F. and Retallack, Gregory J., 2006, Comparison of middle Miocene angiosperm leaf fossils from Cape Blanco with type specimens. Proceedings of the Oregon Academy of Sciences, v. 62, p. 35.

Emerson, Lisa F. and Rempel, Alan W., 2005, Experimental studies of the influence of entrained sediment on ice friction. Eos Trans. AGU, 86(52) Fall Meeting Suppl., Abstract C51B-0287.

Emerson, Lisa F. and Retallack, Gregory J., 2005, A new middle Miocene flora from Cape Blanco, OR. Abstracts with Programs- Geologic Society of America Fall Meeting 37(7), 362.

ACKNOWLEDGMENTS

Brendan Toch, my husband, was a bottomless well of patience. My family and friends were always encouraging, and despite the long road, I never felt abandoned.

TABLE OF CONTENTS

LIST OF FIGURES

LIST OF TABLES

CHAPTER I

INTRODUCTION

The Cape Blanco flora and its paleoclimate implications are the subject of this dissertation. The second chapter establishes the age and depositional environment of the flora. The third chapter describes the flora and includes systematic assignments, photographs of the fossil leaves, and an estimate of the mean annual temperature and mean annual precipitation during late Early Miocene time. The fourth chapter expands the scope of the study to include other Early Miocene floras and the floral data is compared to oxygen isotope based paleoclimate estimates. Together, the second, third, and fourth chapters provide the setting, composition, and importance of the Cape Blanco flora.

The paleomagnetic laboratory analysis and technical figures of the second chapter were produced by my co-authors, Don Prothero and Kristina Raymond. Greg Retallack, a co-author for the second and third chapters assisted in all facets of the work, including idea development, data collection, data analysis, and editing.

CHAPTER II

RADIOMETRIC AND PALEOMAGNETIC DATING OF AN EARLY MIOCENE

FOSSIL FLORA FROM CAPE BLANCO, SOUTHERN OREGON COAST

The paleomagnetic laboratory analysis and paleomagnetic technical figures of the

second chapter were produced by my co-authors, Don Prothero and Kristina Raymond.

Greg Retallack, assisted in all facets of the work, including idea development, data

collection, data analysis, and editing. Though they are not co-authors, Robert Duncan

and John Huard at Oregon State University completed the mineral separation and

laboratory analysis for the $^{40}Ar/^{39}Ar$ date.

1. Introduction

Accurate reconstruction of past climates using terrestrial fossils requires

knowledge of the age, provenance, and depositional environment for host rocks. The

Cape Blanco Flora is a macrofossil assemblage used for paleoclimatic estimates

(Emerson and Retallack 2005, Wolfe 1994) and this paper establishes the age and

depositional environment of the rocks that contain the flora. Cape Blanco is the

westernmost extent of the north/south trending Oregon coast, and the sea cliffs southeast

of the cape expose a sequence of Eocene to Holocene sedimentary rocks on the south

limb of an east/west trending anticline (Armentrout 1980). The axis of the anticline is 1

km north of the cape (Figure 1). Here, emphasis is placed on a 7.5 m bed of redeposited

pumice-rich lapilli tuff that contains the fossil flora. Paleomagnetic stratigraphy,

calibrated by a single-crystal ^{40}Ar/^{39}Ar date, constrains the age and tectonic rotation of
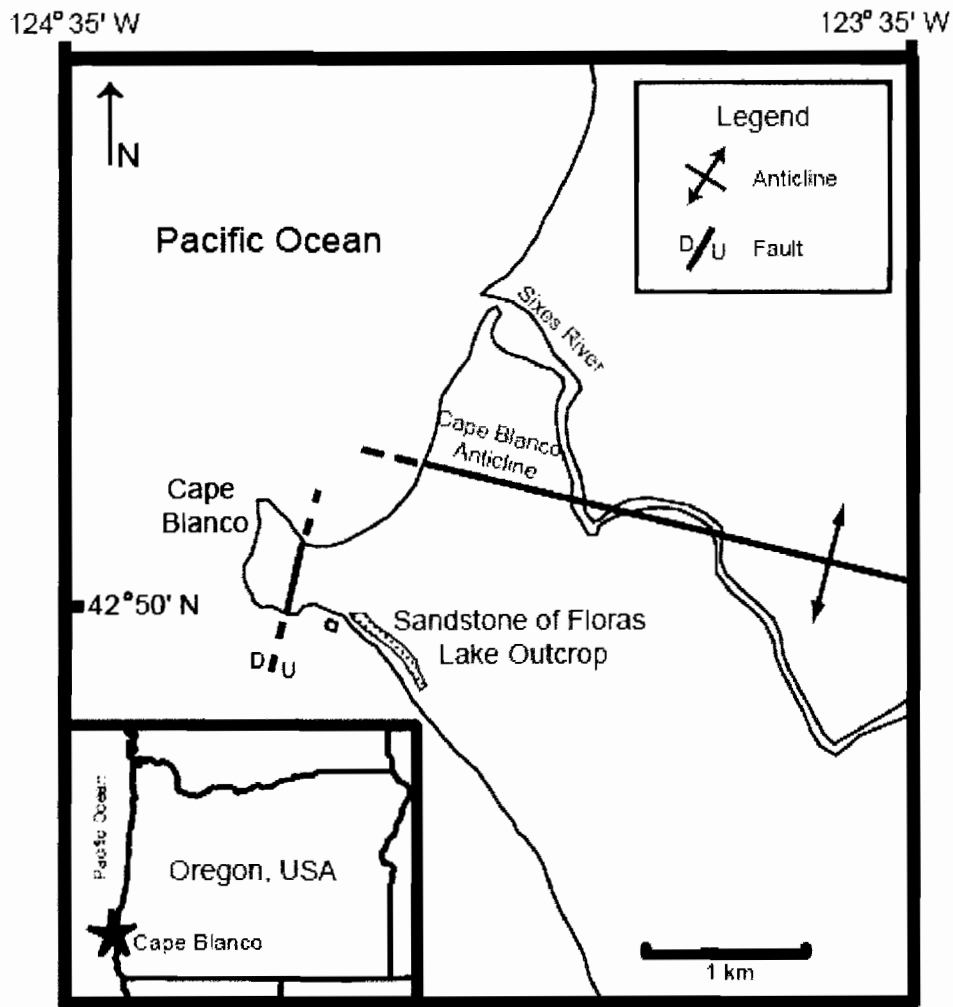
Figure 1: Location map for sandstone of Floras Lake outcrop, modified from Kelsey (1990) and Addicott (1980). For detailed bedrock geology refer to Dott (1962) and for detailed terrace maps refer to Kelsey (1990).

the sediments. Whole rock XRF analysis of the tuff and the adjacent marine sandstones

aid in determining provenance. Sedimentary structures refine the depositional

environment for the tuff bed. Combined, these results serve as a guide to volcanic source

terrane, tectonic setting, and ancient environment of the fossil flora.

Cape Blanco lies near the intersection of three geologic provinces (Figure

2): the subducting Gorda plate, the accreted and metamorphosed Mesozoic Klamath
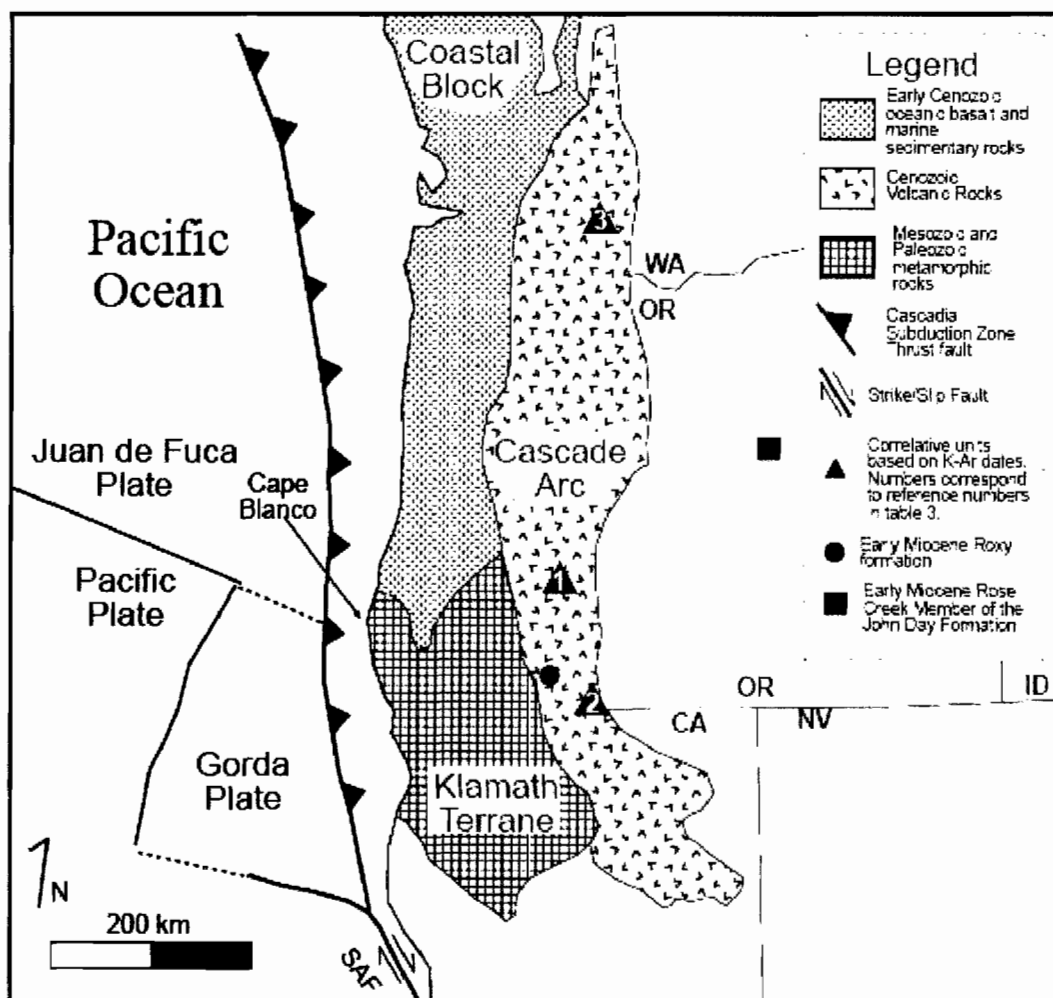
Figure 2: Map of the Pacific Northwest showing tectonic terranes relevant to the history of Cape Blanco. Continental province base map modified from Wells and Heller (1988) and oceanic plate boundaries modified from Dziak et al. (2001). Multiple samples are included in the correlation points because they are too close together to differentiate at this scale. SAF: San Andreas Fault, OR: Oregon, WA: Washington, CA: California, NV: Nevada, ID: Idaho

Terrane and the Tertiary marine basins of the Coast Ranges. The tectonic setting is complex, and addressing uncertainty regarding the areas tectonic history also motivated this study. Cape Blanco has the shortest trench normal distance of the Oregon coast (Miller et al. 2001) and the age of the Gorda Plate at the trench west of Cape Blanco is 6 Ma (Wilson 1989). The accreted Mesozoic rocks of a broadly defined Klamath Terrane have their most northerly coast outcrop at Cape Blanco. The Siletzia terrane thought to underlie the Cenozoic sediments of the Oregon coast range and Willamette Valley has its most southward extent just north of Cape Blanco (Wells et al. 1998). Geological refinement of this section allows for increased precision in the volcanic and tectonic models of the region.

2. Geologic Setting

The northernmost exposure of accreted Mesozoic rocks along the Oregon Coast is at Cape Blanco (Kelsey 1990), and the Jurassic Otter Point sandstones and mudstones (Dott 1962, 1971, Koch 1966) are the resistant rocks of the headland. Unconformably overlying the Otter Point Formation are Cenozoic deposits that have been offset by roughly north trending normal faults (Dott 1962) and folded by the Cape Blanco anticline (Diller 1902, Kelsey 1990). The southern limb of the east-west trending anticline exposes a sequence of SE dipping sedimentary rocks; Eocene Roseburg formation shale (Armentrout et al. 1983, Bandy 1950), early Miocene sandstone of Floras Lake (Addicott 1980, 1983; Armentrout 1980), late Miocene Empire sandstone (Armentrout et al.,1983; Diller 1902), Pliocene Port Orford sandstone (Baldwin 1945), and a flight of Pleistocene

marine terraces (Bockheim et al. 1992, 1996; Diller 1902; Janda 1969; Kelsey 1990). The dip of each unconformity-bound unit (Durham 1953) decreases with age, indicating that the structure has been active since the deposition of the sandstone of Floras Lake (Kelsey 1990). The fault at the neck of the cape brings down late Miocene Empire Formation sandstone which forms the buff colored cliffs that are the source of Cape Blanco's name (Dott 1962).

This study focuses on the 158 m thick Burdigalian (Addioctt 1976, 1980, 1983) sandstone of Floras Lake (Figure 3) which is punctuated by a 7.5 meter thick tuff bed (Figure 4). Previous Miocene age estimates were based on molluscan biostratigraphy (Addicott 1976, 1980, 1983; Allison and Addicott 1976; Moore 1963; Moore and Addicott 1987). The paleoecology of those assemblages indicated rapid deposition along a NW trending rocky coast (Leithold and Bourgeois 1983). Leithold and Bourgeois (1983) subdivided the Sandstone of Flora Lake into four units; the conglomeratic sandstone unit, the pebbly sandstone unit, the tuff, and the sandstone unit (Figure 3). The fining-upward trend seen in these units records a transgressive sequence with a continuous increase in depositional depth from intertidal at the bottom to below stormweather wave base at the top (Addicott 1983, Leithold and Bourgeois 1983). The apparent deepening was interrupted by the deposition of the tuff and was attributed to volcanically induced uplift (Leithold and Bourgeois 1983). Here we closely examine the tuff bed in order to better interpret the fossil flora.
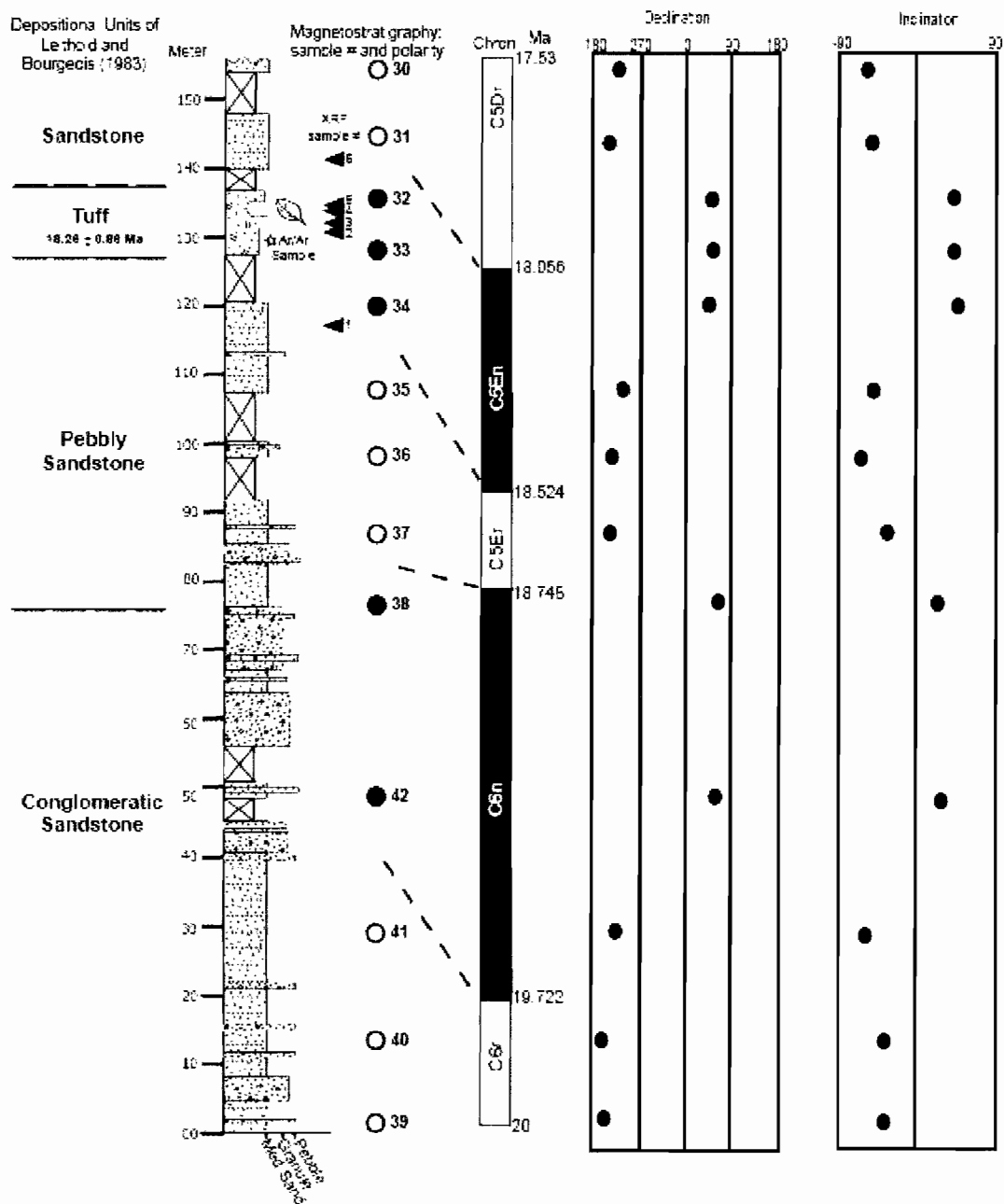
Figure 3: Stratigraphic section of sandstone of Floras Lake with sample locations for XRF and paleomagnetic stratigraphy. Black circles have normal polarization and white circles are reversed. Leaf symbol indicates the location of the fossil flora. Unexposed portions of the section are marked by crossing lines. Assigned polarity zones, inclination, and declination results are on the right.
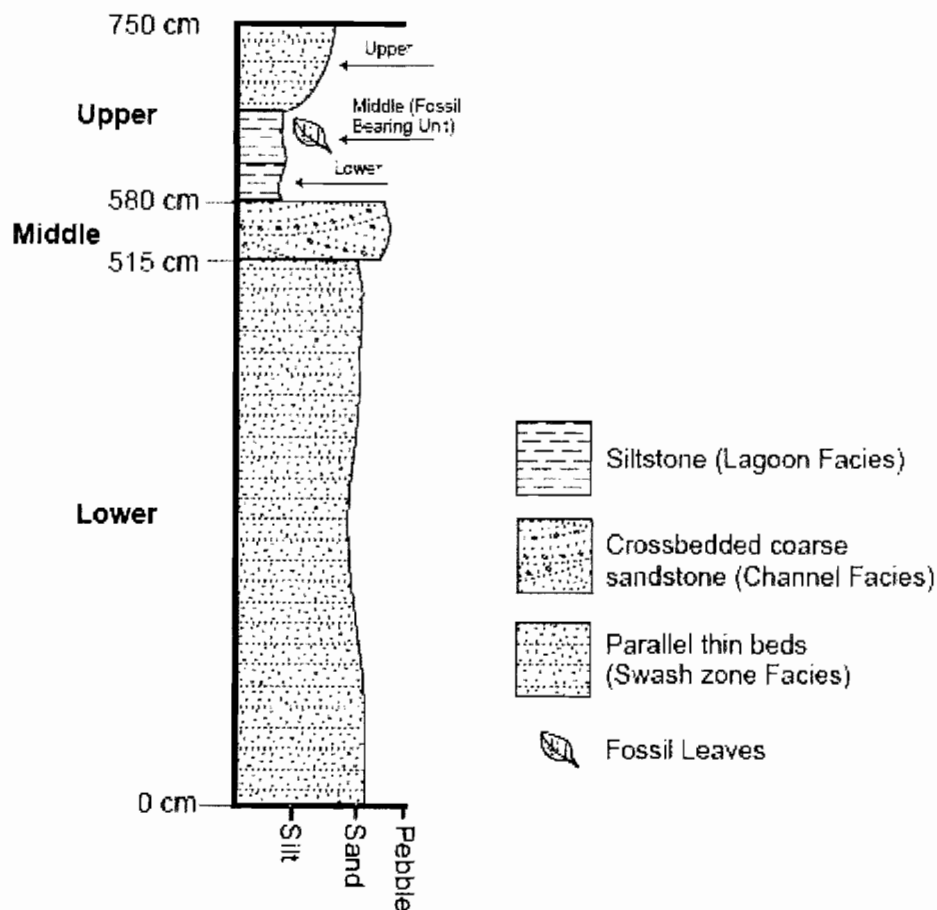
Figure 4: Stratigraphic section of tuff with three zones; upper, middle, and lower. Leaf symbol indicates location of fossil bearing unit.

3. Sedimentary Environment of the Tuff

3.1. Methods

The section is a sea cliff exposure intermittently interrupted by landslides (Figure 3). The section was measured using the eye-height method and grain size and meter scale observations of sedimentary structures confirmed the descriptions of Leithold and

Bourgeois (1983). Grain size and sedimentary structures were recorded for the tuff bed with 0.1 m precision.

3.2. Tuff Outcrop Results

The 7.5 m tuff is a thick, gray, erosion resistant unit composed of a series of even and parallel tabular beds that vary in thickness from a few millimeters to nearly a meter (Figure 4). Sand sized grains are sub-angular and granules are mainly pumice. We divide the tuff into three units; lower, middle, and upper (Figure 4, 5A). These units are evaluated separately and then combined to construct a depositional model for the tuff bed.

The lower tuff unit (0-515 cm) is composed of parallel laminated thin (0.2 cm to 2 cm) beds (Figure 5B). These beds are massive with the exception of a small 3 cm trough cross bed and a 30 cm exposure of ripple cross lamination. There are two distinct bed types within the lower tuff unit based on grain size: uniform and bimodal. Uniform beds are sandy and very well to well sorted. Bimodal beds contain sand and fine pebble gravel (up to 2 cm) pumice grains. This rock fractures conchoidally and does not split evenly on bedding planes. The lower contact of the tuff is obscured.

The middle tuff unit (515-580 cm) is well sorted, sub-angular, coarse grained, trough cross-bedded sandstone (Figure 5C). The bi-directional cross-bedding is truncated at a high angle and the contact with the underlying lower tuff is abrupt and erosional.

The upper tuff unit is subdivided into three sub-units , including a central fossil-bearing unit. The sub-units are: lower (580 to 615 cm), middle (fossil leaf bearing) (615-

655 cm), and upper (655-750). The lower sub-unit of the upper tuff is 15 cm of massive

siltstone overlain by 5 cm of parallel laminated coarse grained thin beds similar to the

basal tuff. The lower contact is gradational and the siltstone has a few interbedded very

fine sand beds with some lenses of coarser sand to granule material. The middle sub-unit

is a massive siltstone and the contact between the lower and middle sub-units is abrupt.
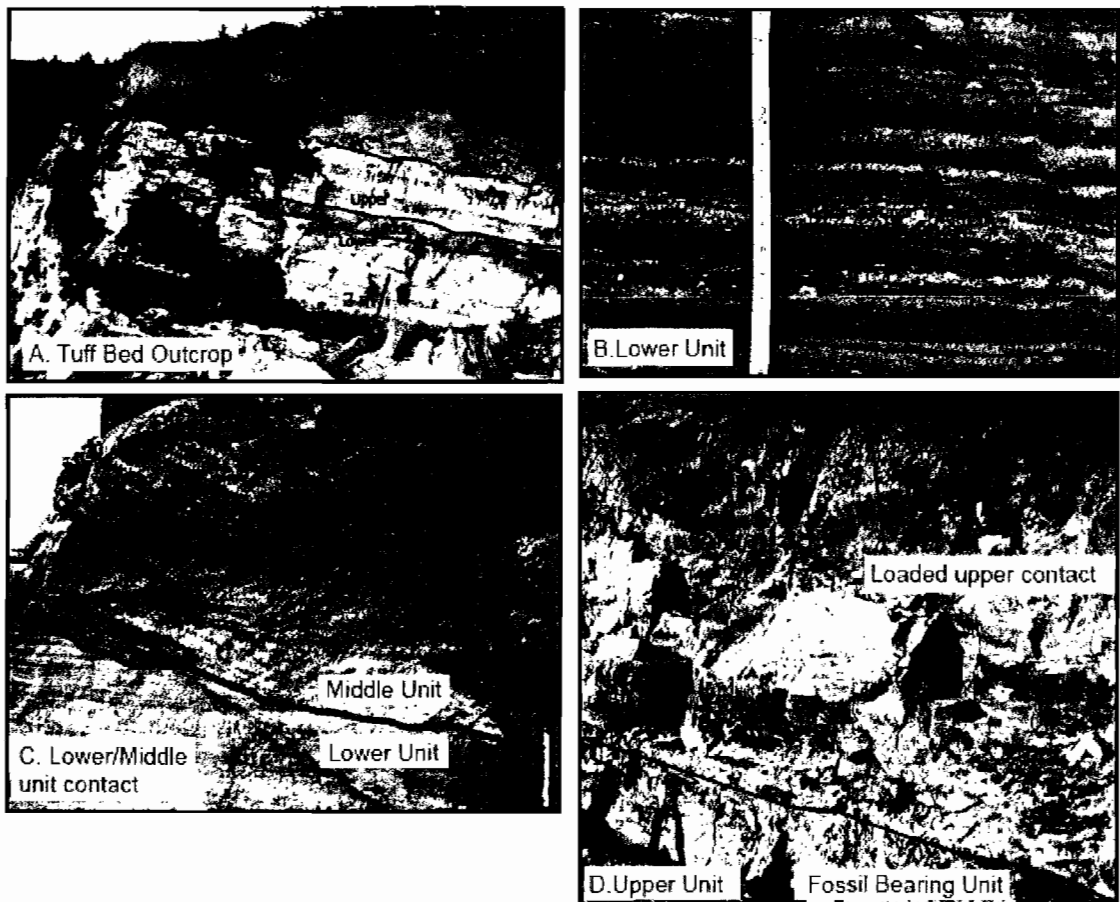
Figure 5: Photographs of tuff bed outcrop. A: outcrop with scale bar, B: lower unit with planar bedding, C: Lower/Middle contact with hammer on right for scale, D. Upper unit with hammer for scale.

The upper sub-unit is a medium grained parallel laminated sandstone with beds varying from 0.5 cm to 15 cm thick. The contact between the upper and middle sub-units is abrupt and planar and the contact between the tuff and the overlying marine sands is loaded.

3.3. Tuff Outcrop Interpretation

The sedimentary structures, rounded granules, predominantly sand sized sediments, and thin planar beds in the lower sub unit of the tuff unit indicate remobilization of sediment rather than direct pyroclastic base surge or airfall on land or into water. These sediments lack dune forms of base surge and graded beds typical of airfall into water (Cas and Wright 1987). The coarse sand is evidence that the sediment was remobilized through traction by water. Evidence of bioturbation is absent indicating rapid deposition, and given the difficulty of fracturing the rock along bedding planes and thus the inferred absence of parting lineation it is likely that the beds were deposited in the lower flow regime (Tucker 2003). Such criteria are met in the swash zone along the shore line (Clifton et al 1971). The trough cross bedding in the middle part of the tuff suggests complex dunes of channeled flow (Selley 2000). We interpret it to be the trough cross-bedded facies of barred nearshore system (Hunter et al. 1979) or a channel on a prograding delta (Reading and Collinson 1996). The massive siltstones are interpreted as lagoonal deposits that trapped fine-grained sediment and floating leaves. The association of swash zone, channeled flow, and lagoon indicate deposition in small barred estuary or a delta.

The abrupt shallowing that occurs at the base of the tuff as well as the thickness

(7.5 m) of the tuff layer suggest that it was the product of at least a moderate size

eruption. Grain size and uniformity suggest this tuff bed was in the distal zone of

volcanic deposition (Vessel and Davies 1981, Scott 1988). The distal zone can extend

from 40-120 km downstream from the volcanic source (Orton 1996, Smith 1988).

Because of the abundant pumice, we infer that the tuff was derived from a Plinian

style volcanic eruption. Such an eruption would have provided a large amount of easily

remobilized sediment to drainage networks supplying sediment to this shallow marine

system. Such rapid inputs of sediment can quickly fill available accommodation space at

the paleoshoreline and cause shallowing and progradation. Stream aggradation was

observed at Mt. St. Helens following the 1980 eruption (Scott 1988) and in Guatemala

following the 1902 eruption of Santa Mariá. In Guatemala, volcanically derived

sediment raised the river bed 10-15 m and an elongate deltaic platform prograded 7 km

(Kuenzi et al. 1979). A similar process likely led to the shallow depositional

environment that is recorded in the tuff bed in the sandstone of Floras Lake. The

aggraded primary stream may have dammed smaller drainages creating lakes. Such lakes

may have assisted in the mechanical size sorting of the remobilized volcanic products by

impounding the coarser fractions and leaving ash and leaves in suspension. When the

lakes were subsequently breeched by headwall erosion or a large precipitation event,

large plugs of ash and leaves could have been remobilized downstream. We call upon an

increase sediment supply as the mechanism for shallowing as opposed to volcanically

induced uplift (Leithold and Bourgeois 1983) because the distance to a plausible source of the tuff is at least 100 km (see section 5.3).

4. ^{40}Ar/^{39}Ar Dating of the Tuff

4.1. ^{40}Ar/^{39}Ar Methods

Two fresh tuff samples were collected in the lower sub unit of the tuff and sent for analysis by Robert Duncan and John Huard at Oregon State University. A sample of plagioclase phenocrysts and hornblende phenocrysts each with a total mass of 50-100 mg as well as FCT-3 biotite monitors (standard age of 28.03 ± 0.18 Ma after Renne et al., 1994) were wrapped in Cu-foil and stacked in evacuated quartz vials and irradiated with fast neutrons for 6 hr in the core of the 1MW TRIGA reactor at Oregon State University. Incremental heating experiments were performed using the MAP215/50 mass spectrometer. The measured argon isotopes (^{40}Ar, ^{39}Ar, ^{38}Ar, ^{37}Ar, and ^{36}Ar) were corrected for interfering Ca, K, and Cl, nuclear reactions (McDougall and Harrison, 1999) and for mass fractionation. Apparent ages for individual temperature steps were calculated using ArArCALC software (Koppers, 2002) assuming an initial atmospheric ^{40}Ar/^{39}Ar value of 295.5, and reported uncertainty (2σ) includes error in regression of peak height measurement, in fitting the neutron flux measurements (J-values), and uncertainty in the age of the monitor. The ^{40}Ar/^{36}Ar normal isochron intercepts confirm that there was no excess Ar in the samples. Plateau ages are the average of concordant step ages, comprising most of the gas released, weighted by the inverse of their standard errors. The decay constants used were $\lambda\varepsilon = 0.581$E-10/yr and $\lambda\beta = 4.963$E-10/yr.

4.2. $^{40}Ar/^{39}Ar$ Results

Of the two samples, only plagioclase yielded a reliable plateau age (Figure 6,

Table 1). The hornblende age was unreliable because of a low amount of original K.

The weighted plateau age of plagioclase is 18.24 ± 0.86 with a MWSD of 0.82. The

plagioclase age values for each step are within the error range of all other steps indicating

a valid age determination.
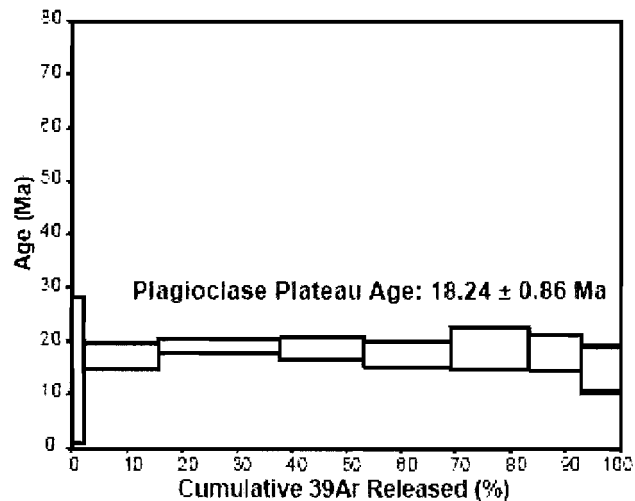
Figure 6: Plagioclase cumulative Argon release plateau. Weighted Plateau age 18.24 ± 0.86 Ma; Total Fusion 17.88 ± 1.03; Normal Isochron 16.28 ± 2.55; Inverse Isochron 18.45 ± 1.23; MSWD 0.82.The weighted plateau age is favored because it has the smallest error.

Table 1: Analytical Data for Radiometric Dates

Sample	Plateau age (Ma)	2 σ error	Total Fusion Age (Ma)	2 σ error	MSWD	Normal Isochron age (Ma)	2 σ error	40Ar/36Ar normal isochron	2 σ error	J
Plagioclase	18.24	0.86	17.88	1.03	0.82	16.28	2.55	309.66	172.16	0.0021259
Hornblende	11.43	6.46	13.78	9.82	0.26	5.89	14.85	301.58	14.62	0.0021169

5. Provenance of the Tuff

5.1. XRF Methods

The purpose of X-ray florescence analysis was to determine chemical differences between the tuff and the surrounding sandstone, and to identify a possible volcanic source for the eruption. We sampled the least weathered rock available within the tuff and approximately 10 meters above and below (Figure 3). The whole-rock samples were then analyzed by ALS Chemex of Vancouver, BC, using CANMET standard SDMS2 with FeO by Pratt titration.

5.2. XRF Results

The X-ray florescence results in weight percentages were normalized for material lost on ignition (LOI) and results are shown in Table 2. There was a higher loss on ignition (LOI) from the tuff samples (sample numbers: 2,3,4 and 5), compared with marine sandstones. This difference can be related to devitrification and hydration of volcanic glass in the interval between airfall and redeposition and/or a greater amount of organic matter in the tuff.

Table 2: XRF Results[a]

Sample #	SiO2	Al2O3	Fe2O3	CaO	MgO	Na2O	K2O	Cr2O3	TiO2	MnO	P2O5	SrO	BaO	FeO	Total	LOI
6	71.61	14.07	4.15	2.31	2.26	2.42	2.42	0.01	0.51	0.02	0.09	0.04	0.07	3.01	93.66	6.32
5	70.42	15.94	3.41	1.48	2.59	3.61	1.94	0	0.4	0.03	0.08	0.02	0.07	1.16	99.45	10.3
4	69.91	16.1	3.61	2.26	2.98	2.89	1.59	0	0.46	0.03	0.08	0.03	0.06	1.37	98.7	12.1
3	71.51	15.46	3.29	1.72	1.96	3.38	2.05	0	0.42	0.05	0.09	0.02	0.07	1.16	98.85	9.99
2	70.47	16.46	3.34	1.68	2.77	2.79	1.81	0	0.47	0.03	0.08	0.02	0.07	1.51	99.86	12.25
1	71.83	13.25	4.47	2.29	2.44	2.56	2.11	0.05	0.72	0.04	0.09	0.05	0.09	1.99	99.74	4.26
An. Er.	2.71	0.83	0.4	0.22	0.18	0.11	0.13	-	0.06	0.03	0.04	-	-	-	n/a	0.35
Tuff Ave	70.58	15.99	3.41	1.79	2.58	3.16	1.85	0	0.44	0.04	0.08	0.03	0.07	1.3	n/a	n/a
Tuff S.E.	0.33	0.21	0.07	0.17	0.22	0.2	0.1	0	0.02	0	0	0	0	0.08	n/a	n/a

. [a] Analysis results with analytical error (An. Er.) reported from 10 replicate samples, mean of the four tuff samples (Tuff Ave.) and standard error of tuff samples (Tuff S. E.). The stratigraphic location of samples is shown on figure 3. Dashes indicate that analytical error data was not available.

5.3. XRF Interpretation

The chemical analyses shows that the tuff is chemically distinct from the adjacent marine sandstones and allow for the classification of the tuff as a dacite (Figure 7) using the total alkali and silica method of LeBas et al. (1992). Change in the sediment supply system is observed by comparing the average and standard error of the four tuff values with the measurements from the adjacent sandstones. Between the tuff and the sandstone below the oxides: SiO_2, Al_2O_3, Fe_2O_3, CaO, Na_2O, K_2O, Cr_2O_3, TiO_2, SrO, BaO, and FeO were outside the 95% confidence interval of an average of tuff values indicating that the tuff inundated the source area and the change in sediment supplied to the system was abrupt. The SiO_2, Al_2O_3, Fe_2O_3, CaO, MgO, Na_2O, K_2O, Cr_2O_3, TiO_2, MnO, SrO, and FeO oxide values for the sandstone above the tuff were also significantly different indicating that once the volcanic material was flushed through, the system generally returned to pre-eruptive conditions. However some dilution of the sediments by
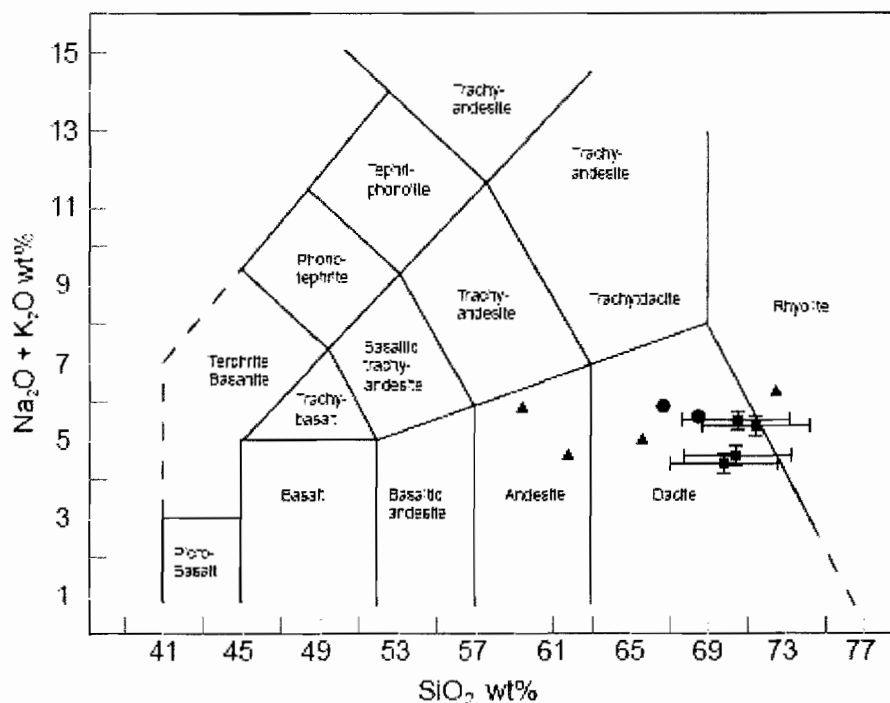
Figure 7: Total Alkali-Silica diagram showing classifications from Le Bas et al (1992). Squares are tuff data, error bars are the analytical error, for the Na2O + K2O the error was summed. Circles are from Verplanck (1985) and triangles are from Mertzman (2000) and correspond with Cascade samples that have Ar/Ar dates that overlap with the Cape Blanco specimens. Errors were not reported and the plotted values are normalized to account for reported totals (Verplanck 1985) and LOI (Mertzman 2000).

controlled redeposition of small amounts of tuff did occur because the SiO_2, Al_2O_3, Fe_2O_3, Cr_2O_3, TiO_2, P_2O_5, SrO and BaO, values for the sandstone above the tuff fall between the values for the tuff and the sandstone below. Thus, most of the tuff was deposited without significant mixing with local sediment. However, tuffaceous sediment continued to be eroded into shallow marine sandstone after eruption diluting the concentration of elements in subsequent sediments.

Given age constraints for the tuff, its source was a part of the 100 km wide predominantly andesitic volcanic belt that spanned the western Cordillera of North America (Christiansen and Yeats 1992), referred to in Oregon as the Early Western Cascades (Priest et al. 1983). Although data on early Miocene Cascade volcanism is limited (Sherrod and Smith 2000), however, information that may permit correlation is of two types. The first type is geologic maps that combine sparse radiometric dating with stratigraphic position to determine age. Rocks of early Miocene age are present in the southern Washington Cascades (Hammond 1980; Swanson 1989), but the most likely correlation is with the compositionally diverse but generally siliceous Roxy formation of the Southern Oregon Cascades (Hladky 1994, 1996, 1999a, 1999b) (Figure 2). The radiometric dates that constrain the age of the Roxy formation are 2-3 million years older than the Floras Lake tuff, though younger potentially correlative units may have been removed by erosion. Geochemical and geochronological studies (du Bray 2006, Hammond 1980, Mertzman 2000, Verplanck 1985) allow for identification of additional correlative units. We identify 10 samples (Table 3) from these studies that may correlate with the tuff bed. The criteria used for identification were that the samples have radiometric dates with two sigma error ranges that overlap with the Floras Lake tuff date and that the samples are classified as andesite or dacite (LeBas et al 1992). The possible correlations are all located within the Cascade Arc (Figure 2).

Table 3: Possible Volcanic Sources [a]

Sample ID	Reference	Age (Ma)	Error (2 σι (Ma)	Age Calculation Method	TAS Classification
M3-36	1	17.8	0.2	K-Ar	dacite
M3-38	1	19.0	0.2	K-Ar	dacite
97-55	2	17.6	0.7	K-Ar	rhyolite
97-54Z	2	17.1	0.8	K-Ar	andesite
97-53	2	19.6	0.6	K-Ar	andesite
JM97-16	2	17.6	0.6	K-Ar	dacite
FRL #4816 (a)	3	18.4	0.3	K-Ar	n/a
FRL #4816 (b)	3	18.9	0.3	K-Ar	n/a
FRL #4817 (a)	3	19.4	1.0	K-Ar	n/a
FRL #4817 (b)	3	20.0	1.0	K-Ar	n/a

[a] Samples that may correlate with the tuff in the sandstone of Floras Lake. Reference 1 is Verplanck (1985), reference 2 is Mertzman (2000), reference 3 is Hammond (1980). Chemical analysis was not provided by Hammond (1980) the rocks are described as dacitic pyroclastic flow deposits. For Verplanck (1985) and Mertzman (2000) samples we normalized the geochemical analysis to account for material LOI and then determined the TAS classification

Quaternary Plinian eruptions of the Cascades produced tephra fallout patterns primarily to the east and deposits rarely reach the coast (Sarna-Wojcicki et al. 1991). Sedimentary units that may correlate with the tuff bed are therefore more likely to be found on the leeward side of the Cascade range. Of comparable age is the Rose Creek Member of the volcaniclastic Eocene to Miocene John Day formation in Central Oregon (Albright et al 2008). The Rose Creek Member contains a number of ash fall tephra beds (Hunt and Stepleton 2004) that may have had the same source eruption as the tuff at Cape Blanco.

Also of note is the amount of chromium in the sandstones (Table 2). The amount of chromium in the adjacent sandstones is much higher than in the tuff. The presence of detrital chromite in sandstone has been used as evidence of onset and development of collision in India and Pakistan because the uplift exposed ultramafic source rocks (Garzanti et al 1996, Warwick et al. 1998). Elevated concentrations of Cr in mudstones

have also been used to identify ultramafic provenance (Garver and Scott 1995). The Klamath Terrane contains ultramafic ophiolites (Harper 1984) and the high Chromium in the sandstones of Floras Lake, excluding the tuff, indicates that the catchment area for the sandstone of Floras Lake likely included the Klamath Terrane.

6. Paleomagnetic Stratigraphy

6.1. Paleomagnetic Method

To better refine the age and tectonic history of the sandstone of Floras Lake, the entire marine sandstone section, including the tuff, was sampled at approximately 15 meter intervals (Figure 3) for paleomagnetic analysis. Oriented block samples were collected at 13 sites spaced approximately 15-meter apart through the 158 meters of section. The surface of the outcrop was scraped to remove the oxidized outer layer, and we also avoided hematite coated fractures. At each site three large block samples were collected with hand tools. The samples were then subsampled into 2.5-cm diameter cores using a drill press or by grinding down the more friable samples with sandpaper and a grinding wheel, then hardening the sample with dilute sodium silicate. From the three large block samples, a minimum of six to eight sub-samples were turned into cores for analysis, except for sites 41 and 42, which were so crumbly that only four sub-samples could be recovered for each site.

Samples were analyzed on a 2G cryogenic magnetometer with a Caltech-style automatic sample changer in the Occidental College paleomagnetics laboratry. After measurement of natural remanent magnetization (NMR), each sample was demagnetized

in alternating field (AF) of 2.5, 5.0, 7.5, and 10.0 mT (millitesla). This enables determination of the coercivity behavior of each sample individually, and demagnetizes multi-domain grains before their magnetism is locked in by heating. After AF demagnetization, each sample was then thermally demagnetized at 50°C steps from 100 to 650°C. This removes overprinting by iron hydroxides such as goethite (which dehydrates to hematite at 200°C), and determines how much of the remanence is held by magnetite and hematite as the blocking temperature of magnetite (580°C) is exceeded.

About 0.1 g of powdered samples of a number of representative lithologies were placed in Eppendorf tubes and subjected to increased isothermal remanent magnetization (IRM) to determine their IRM saturation behavior. These same samples were also demagnetized twice, once after having acquired an IRM produced in a 100 MT peak field, and once after having acquired an anhysteretic remanent magnetization (ARM) in a 100 mT oscillating field. Such data are useful in conducting a modified Lowrie-Fuller test (Pluhar et al. 1991).

Results were plotted on orthogonal demagnetization ("Zijderveld") plots, and the average direction of each sample was determined by the least-squares method of Kirschvink (1980). Mean directions for each sample were then analyzed using Fisher (1953) statistics, and classified according to the scheme of Opdyke et al. (1977).

6.2. Paleomagnetic Results

Representative orthogonal demagnetization plots and are shown in Figure 8. Most of the samples showed a dip-corrected NRM direction either northeast and down (a normal

direction rotated clockwise) or southwest and up (a reversed direction rotated clockwise),

and most of the samples showed only this single component as their vectors decayed to

the origin. A small number of samples showed some overprinting that was typically

removed by 300°C, and then a single component of remanence that decayed to the origin.

The fact that nearly every sample showed a significant drop in intensity during AF

demagnetization indicates that most of the remanence is held by a low-coercivity mineral

such as magnetite; this is consistent with the fact that nearly all the remanence was lost

when the blocking temperature of magnetite (580°C) was exceeded. Thus, it appears that

the samples show a primary or characteristic remanence that is rotated counterclockwise.

The IRM acquisition experiments indicated that the samples contained significant

amounts of magnetite, as the IRM saturated at 300 mT. The Lowrie-Fuller tests indicated

that the grains in the sample were single-domain or pseudo-single-domain, because the

ARM was more resistant to AF demagnetization than the IRM.

The mean directions of all 13 sites were significantly removed from a random

distribution at the 95% confidence level, or Class I sites in the system of Opdyke et al.

(1977) (Table 4). The mean direction for all the normal samples (n = 34) was D = 49.7, I

= 41.0, k = 14.7, α_{95} = 6.6; for the reversed samples, the mean (n = 37) was D = 208.9, I

= -42.3, k = 6.0, α_{95} = 10.5 (Table 4). These mean directions are antipodal within the

error estimates, giving a positive reversal test and showing that the remanence is primary

with most of the overprinting removed (Figure 9).
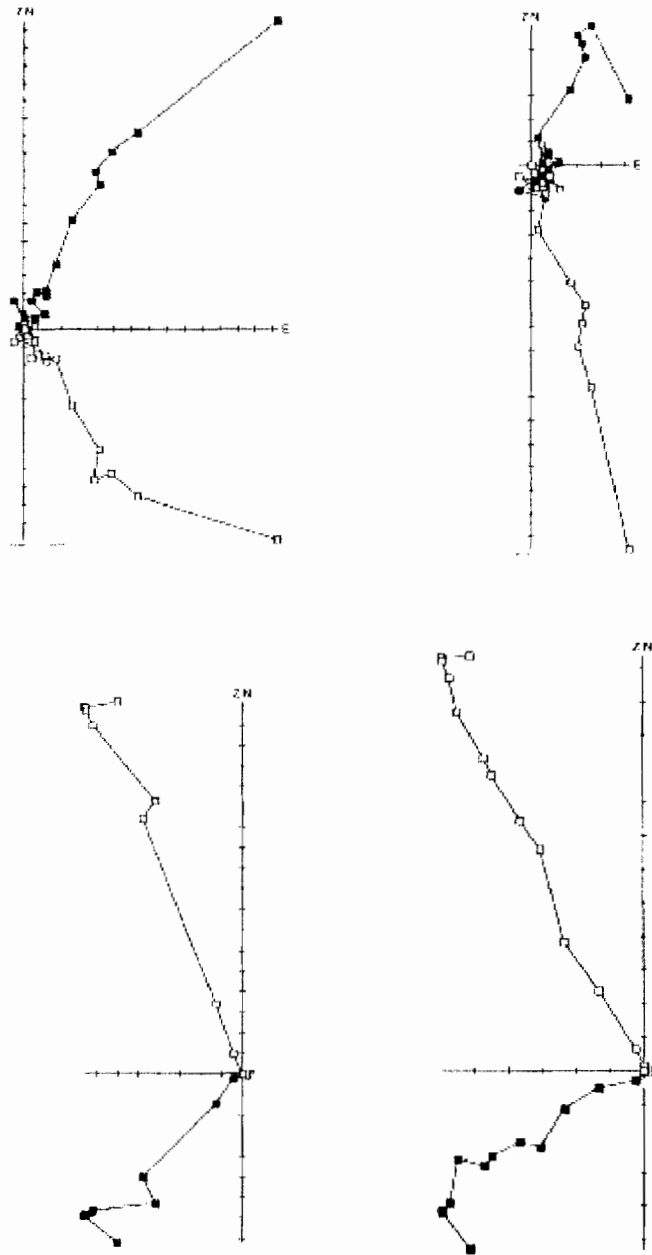
Figure 8: Orthogonal demagnetization ("Zijderveld") plots showing representative results. Solid circles = declination (compass direction); open circles = inclination (up-down component). First step is NRM, followed by 25, 50, 75 and 100 mT AF, then thermal steps from 100° to 650°C in 50°C increments. Top two plots are normally magnetized with slight clockwise rotation; bottom two are reversely magnetized, also rotated. Most of the remanence is held in magnetite, based on low coercivity and loss of magnetization above the Curie point of magnetite (580°C).

Table 4: Paleomagnetic Data [a]

SITE	N	D	I	k	α_{95}
30	7	233.0	-46.9	9.4	20.7
31	6	216.5	-41.2	7.9	25.4
32	8	45.2	45.6	13.2	15.8
33	6	41.9	43.6	11.4	20.7
34	8	38.1	45.5	53.3	7.7
35	7	239.0	-44.8	7.9	22.9
36	8	191.9	-58.4	3.8	32.6
37	8	192.1	26.9	16	14.3
38	6	59.2	33.2	15.8	17.4
39	6	205.9	-35	6.5	28.3
40	4	206.1	-32.2	11.2	28.8
41	4	235.0	-50.1	9.2	32
42	6	64.9	31.1	15.4	17.6

[a] Paleomagnetic data and Fisher statistics. N = number of samples; D = declination; I = inclination; k = precision parameter; α_{95} = ellipse of 95% confidence around mean.

Plotting the magnetic results on the stratigraphic section (Figure 3) yields a magnetostratigraphy with five polarity zones. The basal 40 m of section has reversed polarity, followed by the next 40 m of section consisting of rocks wish normal polarity. From 85 to115 m in the section, the rocks have reversed polarity. Between 115 and140 m in the section (including the dated tuff), the rocks have normal polarity. The uppermost 15 m of section have reversed polarity. Thus we have a R-N-R-N-R sequence of five roughly equal-length polarity zones spanning 158 m of section, and calibrated by the dated tuff near the top.
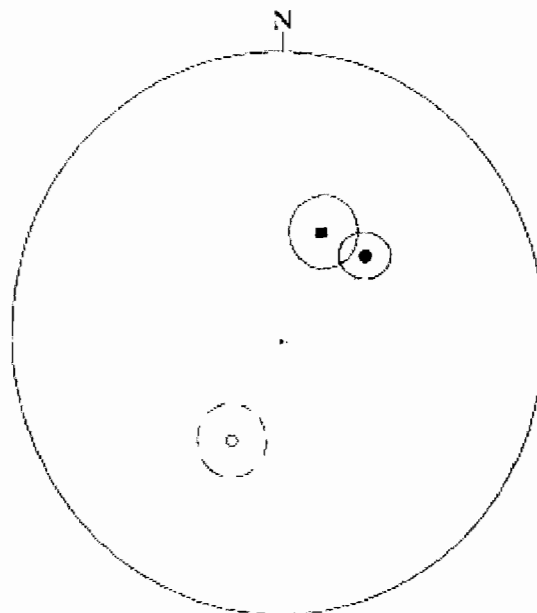
Figure 9: Stereonet of paleomagnetic results showing mean and ellipse of 95% confidence of normal samples (solid dot and circle) and reversed samples (open circle and dashed line). The latter is inverted through the center of the stereonet (solid square and circle), showing that the directions are antipodal, and that the overprinting has been removed.

Inverting the reversed directions and averaging all the vectors yields a formational mean direction of D = 38.0, I = 43.6, k = 6.7, α_{95} = 7.1 (n = 71). This mean is rotated clockwise by about 37.6° ± 7°, degrees from the expected early Miocene cratonic pole (Diehl et al., 1983). This is much less than the 105 ± 5° reported from the middle Eocene Coaledo Formation in nearby Coos Bay, Oregon (Prothero and Donohoo, 2001a), and 106 ± 18° for the lower Oligocene Tunnel Point Formation overlying the Coaledo Formation in Coos Bay (Prothero and Donohoo, 2001b). However, it is much more than the 9.0 ± 8° of clockwise rotation reported from the upper Miocene (6-8 Ma) Empire Formation in Coos Bay (Prothero et al., 2001). Thus, the early Miocene rotation of about 38° clockwise at Cape Blanco is intermediate between the large (greater than 90°)

clockwise Eocene-Oligocene rotations and the small late Miocene rotations reported from the region.

6.3. Paleomagnetic Interpretation

The plagioclase $^{40}Ar/^{39}Ar$ crystal yielding the 18.24 Ma ± 0.86 Ma came from the fourth polarity zone and may correspond with normal polarity chrons C5Dn, C5D*r.1n*, C5En, or C6n (Ogg and Smith. 2004). To determine the preferred age assignment the deposition rate was estimated by dividing the thickness (m) of polarity zones 2, 3, and 4, 42.5m, 32.5m, and 26.5m, respectively, by the duration (Ma) of the possibly correlating chrons. The 23,000 year chron, C5D*r.1n*, produced deposition rates an order of magnitude greater than the adjacent zones and therefore the reversal was likely not captured by the coarseness of our sampling. The other three chrons all yielded reasonable deposition rates and our preferred correlation for zone four is with polarity chron C5En because this chron overlaps with the $^{40}Ar/^{39}Ar$ date.

6.4. Paleomagnetic Discussion

Cenozoic rotation of the Oregon coastal block has been recognized for some time (Simpson and Cox, 1977), and generally the amount of rotation decreases through the Tertiary (Beck and Plumley, 1980; Magill and Cox 1980; Prothero and Donohoo, 2001a,b; Prothero et al., 2001). The tectonic mechanism driving deformation has been attributed to oblique subduction of the Juan de Fuca and associated microplates and expansion of the Basin and Range Province (Wells 1990; Wells and Heller, 1988; Wells

and Simpson 2001; Wells et al, 1998). The rotations observed in our paleomagnetic data are consistent with previously documented clockwise Oregon coastal block rotations. But given the unlikelihood that Cape Blanco is underlain by Siletzia, the post Miocene motion observed at Cape Blanco may reflect dextral shearing (Wells 1990) as opposed to rigid block rotation. Prothero and Donohoo (2001a) also suggested dextral shearing as the rotational mechanism for Eocene deposits 60 km north of Cape Blanco at Coos Bay, Oregon. These long-term geologic observations are supported by modern GPS studies that parse the observed North American plate motion (McCaffrey et al. 2000, Murray and Lisowski 2000, Savage et al, 2000) into interseismic strain caused by a locked zone in the subducting slab and a residual velocity which is consistent with clockwise rotation (Miller et al. 2001) about a Euler pole located along the eastern portion of the Washington-Oregon border (Lewis et al. 2003).

The depositional rates inferred by sediment thickness and the assigned polarity zones vary between 50 and 150 meters per million years. This rate is consistent with that predicted by Leithold and Bourgeois (1983).

7. Conclusions

Our analysis of the sandstone of Floras Lake and the tuff bed within it shows that the shallow marine depositional environment for the sandstone beds (Leithold and Bourgeois 1983) was interrupted by a transient deltaic progradation of redeposited volcanic material which contains the Cape Blanco flora. Isotopic data constrain the age of the plant-bearing tuff to 18.24 ± 0.86 Ma, and we interpret this age as an age of

eruption with near instantaneous redeposition. The eruption took place in the Cascade arc, but a precise source remains undetermined. Paleomagnetic data confirm that the area was rotated clockwise after deposition, likely by dextral shear. The relation between the early Miocene Cascade volcanic arc and the Klamath Terrane was fixed since the early Miocene (Magill and Cox 1977; Wells and Heller 1988) and given the Cascade source and the high Cr_2O_3 in the sandstones it is likely that the source area for the sandstone of Floras Lake extended across the Klamath Terrane which may have been much lower relief at that time (Aalto 2006). The >100 km distance between the likely eruptive center and the site of deposition means that the leaves of the Cape Blanco flora capture the floral diversity and paleoclimate on the coast west of the early Miocene Cascade arc.

The following chapter describes the fossils recovered from the tuff bed.

CHAPTER III

SYSTEMATICS OF THE EARLY MIOCENE CAPE BLANCO FLORA OF

COASTAL OREGON

Greg Retallack assisted in all facets of the work, including idea development, data collection, data analysis, and editing.

INTRODUCTION

Coastal location and radiometric age of 18.26 ± 0.86 Ma (Chapter II) make the Cape Blanco flora important for paleoclimatic and floristic assessment, because previously documented Miocene floras of Oregon, USA, (Table 1) are inland. Coastal records are important because their paleoelevation is constrained and they provide a link between marine records of global climate (Zachos et al., 2001) and inland climate records (Wolfe, 1994; Retallack, 2007). Both records of climate indicate a time of global cooling from late early to middle Miocene peak temperatures. Regional reconstruction of paleoclimate is important to the testing of climate models (Wing and Greenwood, 1993; Wing et al., 2005, Sewall and Sloan, 2006) as well as tectonic reconstructions that call upon climate as a potential driver (Ruddiman, 1997). Furthermore increasing temperature resolution at sea level allows for more accurate interpretation of terrestrial

lapse rate based studies of paleoelevations (Axelrod, 1968, Forest et al. 1999) and

better reconstructions of paleo latitudinal temperature gradients (Miller et al., 2006).

Table 1: Miocene Floras of Oregon [a][b]

Flora	Reference	Age: From listed reference	Status
Lolo Pass	17	Latest Miocene	b
Alvord Creek *	4	Late Miocene	a,b,d
Unity	13	Late Miocene	a,b,d
Vibbert	1	Late Miocene	a,b,d
Mascall *	5, 9	Mid-Late Miocene	a,b,d
Troutdale *	4, 16	10	a,b,c
Faraday	16, 17	11 to 12	b,c
Liberal	16	13	b,c
Molalla	16	13	b,c
Vinegar Creek	17	Late middle to early late Miocene	-
Weyerhauser	16, 17	14-18	b,c
Blue Mountain *	5, 12	Mid Miocene	a,b,d
Cape Blanco	6, 16	Mid Miocene	a,b,c
Jamison	17	Early to Mid Miocene	b
Baker	17	Early to Middle Miocene	-
Hidden Lake	17, Mentioned in 7	Late Early the Middle Late	b
Little Butte Creek	17	Late early to early middle Miocene	b
Skull Spring	17	Late early to early middle Miocene	-
Sparta	17, Mentioned by 7	Late early to early middle Miocene	b
Beulah	2	Miocene (UCMP database)	b,d
Pelton	1	Miocene	a,b,d
Stinking Water *	5	Miocene	a,b,d
Succor Creek *	7, 8, 11, 14	Miocene	a,b,d
Trout Creek *	5, 8, 10	Miocene	a,b,d
Eagle Creek *	16	18-22	b,c
Collawash *	16	18-22	b,c
Forman Point	1	Early Miocene	b
Fish Creek Road	7	?	-
Cascadia	7	?	-
Sandstone Creek	Mentioned in 7, 15	?	-
* Multiple localities			

[a] References: 1 (Ashwill 1983); 2 (Axelrod 1964); 3 (Chaney 1938); 4 (Chaney et al. 1944); 5 (Chaney and Axelrod 1959); 6 (Emerson and Retallack 2005); 7 (Fields 1996); 8 (Graham 1963); 9 (Knowlton 1902); 10 (MacGinitie 1933); 11 (Niklas et al. 1978); 12 (Oliver 1936); 13 (Retallack 2004); 14 (Smith 1932); 15 (Wolfe 1981); 16 (Wolfe 1994); 17 (Wolfe and Tanai 1987);
[b] Status: a) location described; b) location shown on map; c) published climatic information; d) published taxonomy

GEOLOGICAL SETTING

Cape Blanco is located along the southern Oregon coast (Figure 1) and sea cliffs

south of the cape expose a southeast dipping section of Cenozoic sedimentary rocks
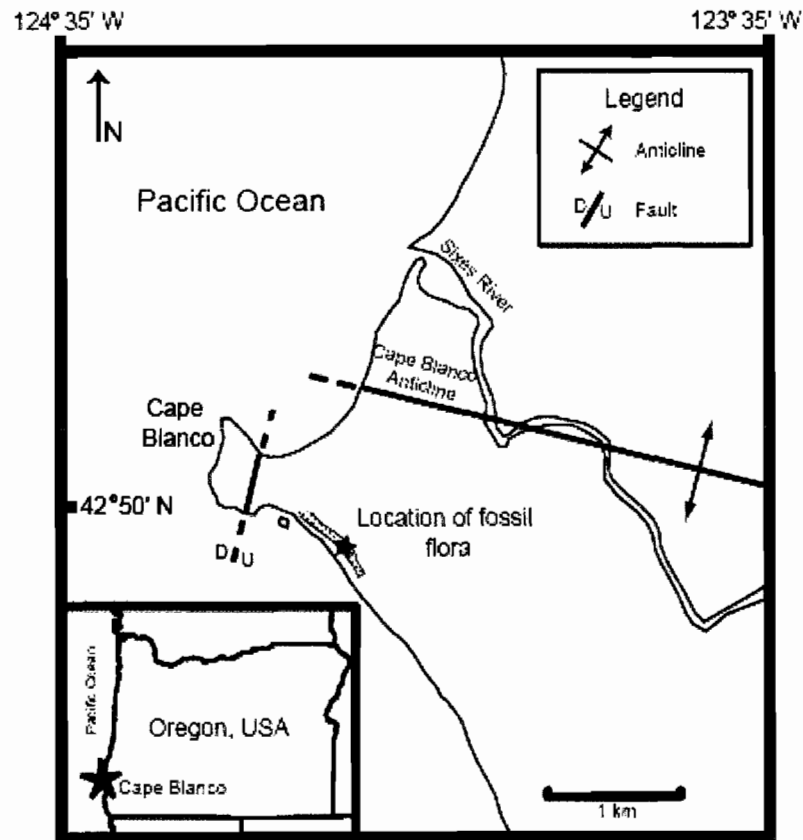
Figure 1: Location map showing location of fossil locality (star). Modified from Kelsey (1990) and Addicott (1980). For detailed bedrock geology refer to Dott (1962) and for detailed terrace maps refer to Kelsey (1990).

(Addicott, 1980). The unconformity bound, early Miocene, sandstone of Floras Lake

contains a 7.5 m thick rhyodacitc tuff bed with leaf bearing beds (Figure 2). The

pumiceous tuff is comparable with others from a Plinian eruptions in the Western

Cascade Arc. Planar bedding and <1 meter scale trough cross bedding within the tuff are

evidence that it was deposited at sea level (Emerson and Retallack 2007). The source
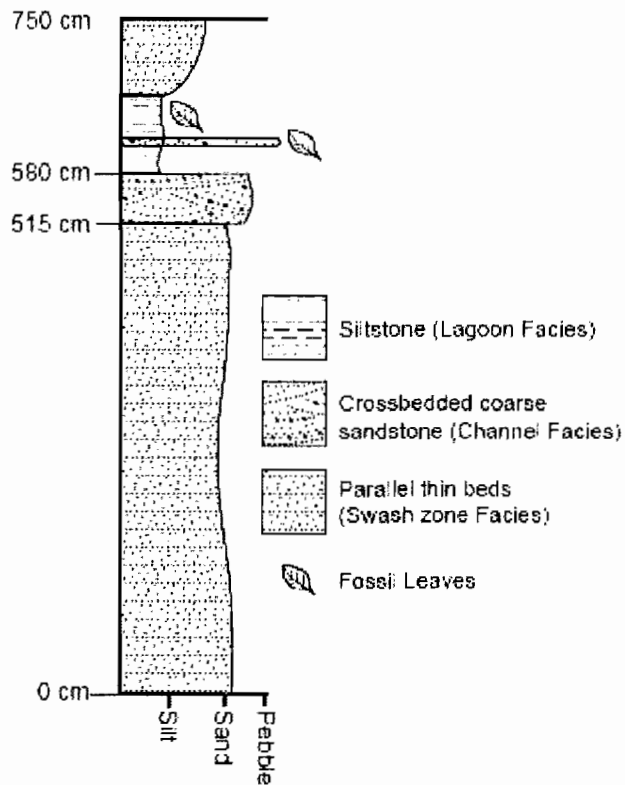
Figure 2: Stratigraphic section of tuff bed with three zones; upper, middle,and lower. Leaf symbol indicates location of fossil bearing unit.
.

eruption may have dammed local catchments. When these lakes and washes were

drained, the plug of ash and leaves was flushed to the shoreline where the fine grained,

leaf laden material settled in a small oxbow lakes on a delta or in lagoons adjacent to

barrier bars. The Cape Blanco flora was discovered and briefly characterized by Wolfe (1994) and noted by Leithold and Bourgeois (1983).

MATERIALS AND METHODS

Megafossil Remains

Abundant new material (687 specimens) was collected for this study from a single quarry in six trips totaling 102 man hours. Rock was removed from the quarry in ~ 40 cm x 40 cm x 40 cm blocks and then broken down into fist sized pieces. The tuff was difficult to break and the leaves were randomly oriented. The majority of leaf fossils were within a single massive, 40 cm thick grey shale and an underlying 10 cm of coarse sand to granule pumiceous tuff bed. This precluded stratigraphic investigations finer than the bed thickness. Coniferous needle litter was predominantly found in the coarse grained, basal, pumice conglomerate. Fossils that had promise of identifiable features were collected and brought to the laboratory for further analysis.

In the laboratory, morphotypes were created to document diversity in the flora. The morphotypes were based on the part of the leaf preserved (eg. apex, base, margin), level of preservation, venation, size, and margin state. As the fossils were considered in the laboratory each was assigned to a morphotype and a total of 115 morphotypes were established. To ensure that the full diversity of the assemblage was captured we created a rarefaction curve (Figure 3) to show the rate of new morphotype establishment. When additional material failed to warrant the establishment of new morphotypes, we were satisfied that we had captured the diversity present in the flora. Well preserved

morphotypes were subsequently assigned fossil names, and in many cases

morphotypes were merged where transitional examples warranted.
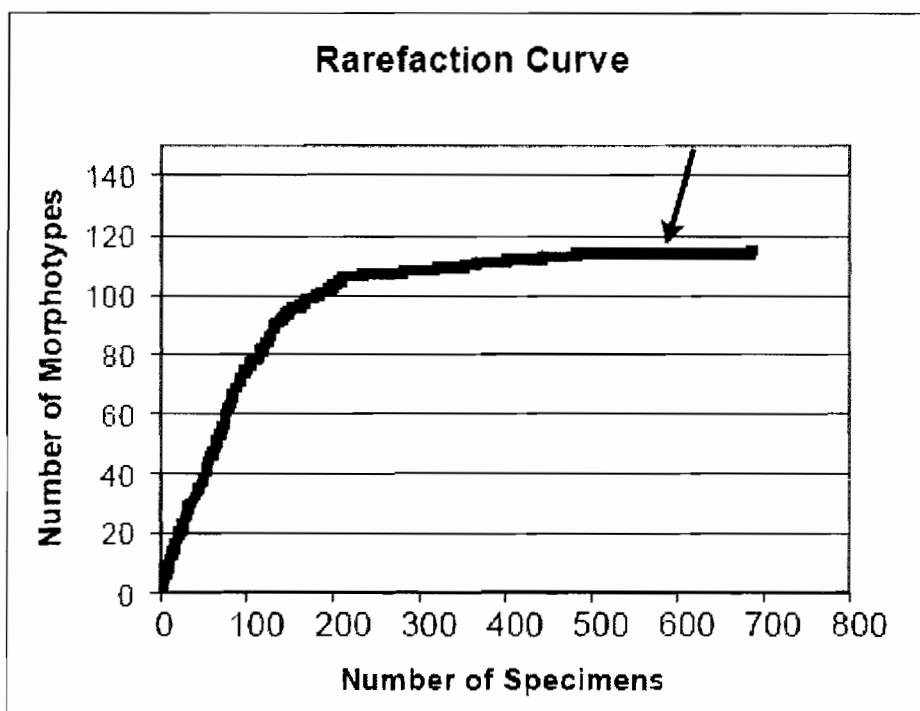
Figure 3: Rarefaction curve documenting the decrease in new morphotype discovery with increasing specimens. The flat portion of the graph (arrow) demonstrates that the morphological diversity present in the flora was captured by our collections.

Photographs for figs 4-10 were taken using a Canon EOS 10D camera with a

macro lens. Images were converted to grey scale and brightness and contrast were

adjusted using Adobe Photoshop 6.0.

No new species were described as a part of this study. Leaf forms that could not

be assigned to a fossil name, but were unique, were assigned numbers and are described

at the end of the section. Specimens included in this study are from two collections; the majority were collected by the authors, as described above, and are housed in the Condon Collection of the Museum of Natural and Cultural History, University of Oregon (UO specimen numbers). The Condon Collection specimens were supplemented by 73 specimens from the Wolfe collections on loan from the Smithsonian, Washington D. C. (W specimen numbers) and are noted when figured.

We retain the usage of fossil names in this study and do not attempt to unambiguously associate the fossil species with a modern equivalent. However, we recognize the similarity of fossil species with extant plants and rely on the nearest living relatives assigned by previous workers to aid in the floristic interpretation of the flora. The systematic assignments are organized by order and the families are assigned to orders following USDA (2009).

SYSTEMATICS

Order— Equisetales

    Family—Equisetaceae Michx. ex DC.

    Genus—*Equisetum* sp.

    Referred specimens— UO F 38064 (Fig.4A); UO F 38088A (Fig. 4B)

    Description— *Equisetum* is recognized by longitudinally ridged axes, separated by nodes. Only stems were found. Stems were 1-2 cm wide with nodes every 2.5 cm.

Order— Pinales

Family—Pinaceae

Genus—*Pinus*

Species—*Pinus tiptoniana* Chaney and Axelrod, 1959, p. 142; pl. 13, figs. 6, 7.

Referred specimens— UO F 38089A (Fig.4C).

Description—*Pinus tiptoniana* is represented by a single specimen which we identify as a two needle bundle because of thickening at the base that we interpret as a fascicle. The needle is 15 cm long and each needle is 2 mm wide. Longitudinal ridges run the length of the needle. This is similar to *Pinus ponderosoides* Axelrod because both are long needled pines, however *Pinus ponderosoides* has three needles per bundle and a more prominent fascicle.

Uncertain Affinity— Cone unit

Referred specimens— UO F 38090A (Fig.4L).

Description— The shape of this specimen is similar to a cone unit of a conifer such as *Pinus* but is too abraded and frayed for secure identification.

Uncertain Affinity— Charcoal

Referred specimens— UO F 38091 (Fig. 4D), UO F 38093 (Fig. 4G), UO F 38094 (Fig. 4M), UO F 38095 (Fig. 4F).

Description— Many rounded charcoal pieces up to a few centimeters in the long axis direction were found in the coarse grained layer. Vessels could not be identified in
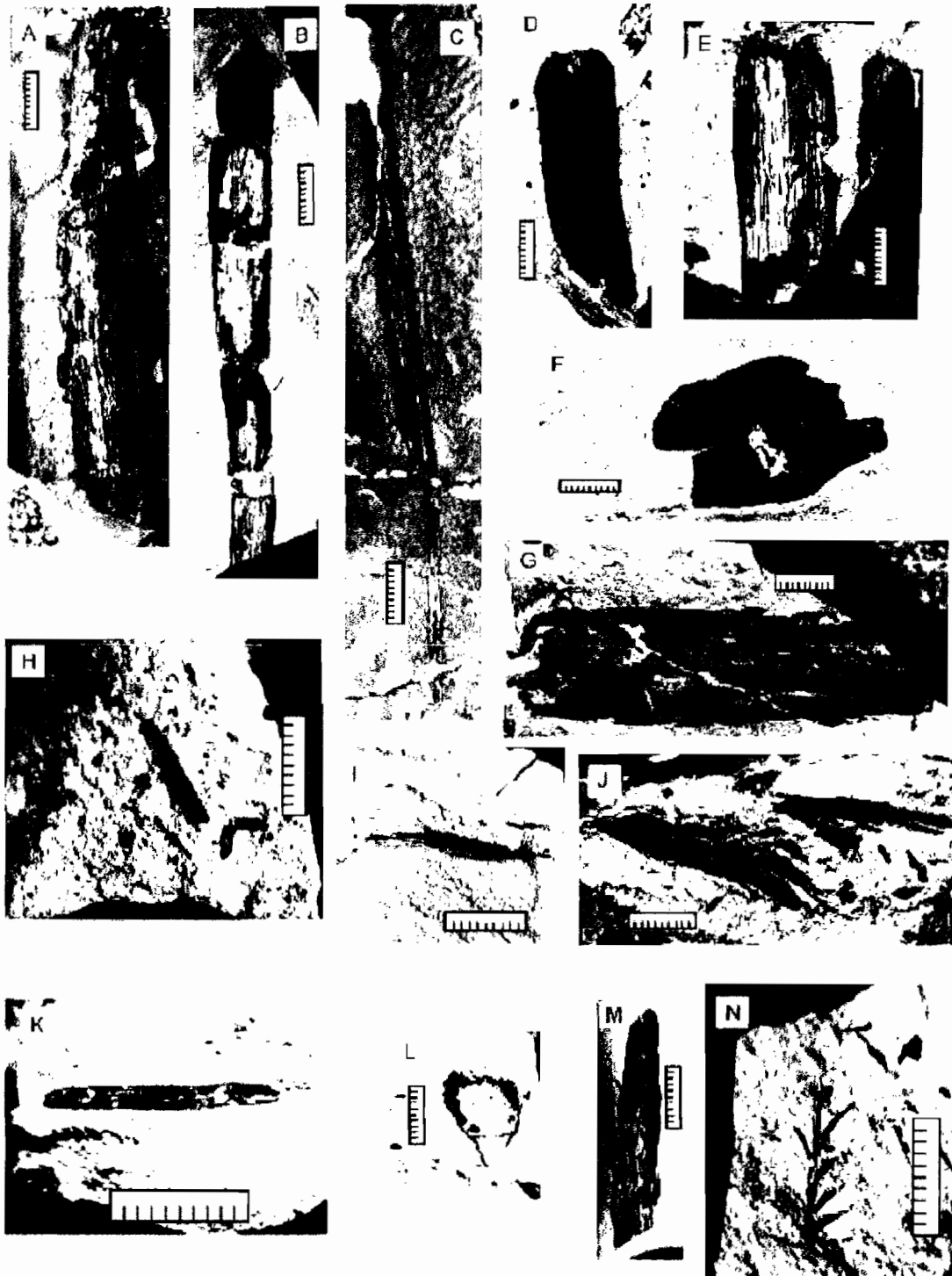
Figure 4: Cape Blanco fossils, orders Equisetales and Pinales, scale bar is 1 cm. **A.** Equisetum sp. UO F 38064 **B.** Equisetum sp. UO F 38088 A, arrow at node. **C.** Pinus tiptoniana UO 38089A. **D.** Charcoal, UO F 38091. **E.** Shredded wood, UO F 38104. F. Charcoal, UO F 38095. **G.** Charcoal, UO F 38093. **H.** Needle, UO F 38114. **I.** Shredded wood, UO F 38101B. **J.** Shredded wood, UO F 38103. **K.** Needle, UO F 42033A. **L.** Cone Unit, UO F 38090A. **M.** Charcoal, UO F 38094. **N.** Splayed needles, UO F 38105B.

the samples suggesting it is conifer wood. There was a range in sizes from a few cm, UO F 38093, to a piece that was larger than 10 cm, UO F 38092.

Uncertain Affinity— Needles

Referred specimens— UO F 38114 (Fig. 4H), UO F 42033A (Fig. 4K).

Description— Many disaggregated pieces of coniferous debris were found in the coarse grained, basal, pumiceous layer. A few 1-2 cm solitary needles with a midrib, UO F 38114 and UO F 42033, resemble *Abies* needles although limited material precluded specific assignment. Other, larger needle pieces may be fragments of *Pinus tiptoniana*.

Uncertain Affinity— Shredded wood

Referred specimens— UO F 38101B (Fig. 4I), UO F 38103 (Fig. 4J), UO F 38104 (Fig. 4E).

Description— Compressed wood is dark and thick, but lacks the equant rounded shape of the charcoal morphotype. The ends of the pieces are frayed giving the wood a shredded appearance. Modern wood of cedar (*Thuja)*, and pine (*Pinus)*, shreds in a comparable way as it weathers.

Uncertain Affinity— Splayed needles

Referred specimens— UO F 38105B (Fig. 4N).

Description— These specimens have needles attached to a stem and are likely part of a conifer short shoot, similar to Douglas fir (*Pseudotsuga menziesii*), and spruce (*Picea*).

Order—Typhales

Family—Typhaceae

Uncertain Affinity— *Typha* sp.

Referred specimens— UO F 38108A (Fig. 5A), UO F 38110 (Fig. 5B).

Description— These specimens showed longitudinal parallel venation and did not

have relief. No connected stems, nodes, or sheaths, characteristics of Poaceae, were

found. The laminae were 2-5 mm wide.

Order— Salicales

Family— Salicaceae

Genus—*Populus*

Species— *Populus eotremuloides* Knowlton.

Populus eotremuloides Knowlton, 1898, . 725; pl. 100, figs. 1, 2; pl. 101, figs. 1, 2.

Populus eotremuloides Chaney and Axelrod 1959, p 151; pl. 17, fig 4.

Populus eotremuloides Axelrod 1991, p 41; pl. 6, figs. 1, 3, 8.

Populus eotremuloides Buechler et al, 2007, p 322; Fig. 3C.

Referred specimens— UO F 38118A (Fig.5C), UO F 38119A (Fig. 5D), UO F

38121 (Fig. 5E), UO F 38120 (Fig. 5F).

Description— Suprabasal actinodromous primary venation is a diagnostic

character of *Populus*. The two *Populus* species observed at Cape Blanco are

distinguished by the margin with *P. eotremuloides* tending toward an entire to very finely

serrate margin and *P. lindgreni* having a crenate margin with pronounced teeth. This

corresponds with the serration observed on the often cited nearest living relative of this

species, *Populus trichocarpa*, which has since been revised to, *Populus balsamifera* L.

ssp. *trichocarpa* (Torr. & A. Gray ex Hook.)(USDA 2009). Many leaf fragments were

also assigned to this species because of the unique margin, apex angle, and venation

pattern.

Family— Salicaceae

Genus—*Populus*

Species— *Populus lindgreni* Knowlton.

Populus lindgreni Knowlton, 1898, p. 725; pl. 100, fig. 3.

Populus lindgreni Chaney and Axelrod, 1959, p. 151; pl. 17, fig. 1-3.

Populus lindgreni Buechler et al, 2007, p. 322; Fig. 3E.

Referred specimens— W 50 (Fig. 5G), W 51 (Fig. 5H).

Description— Buechler et al. (2007) included *Populus voyana* Chaney and

Axelrod (1959) in *P. lindgreni* because the evidence used by Chaney and Axelrod (1959)

to split *P. voyana* from *P. lindgreni,* petiole and midrib thickness, could be explained by

natural variation within the species. Fields (1996) did not document *P. lindgreni* at

Succor Creek, but in his discussion of *P. voyana* he recommended the separation. We

assigned our specimen to the priority name, *P. lindgreni* because our specimen,

particularly the teeth, most closely resembles *P. lindgreni* Chaney and Axelrod (1959 pl.

17, fig 2). We follow Chaney and Axelrod (1959) who suggested that the nearest living
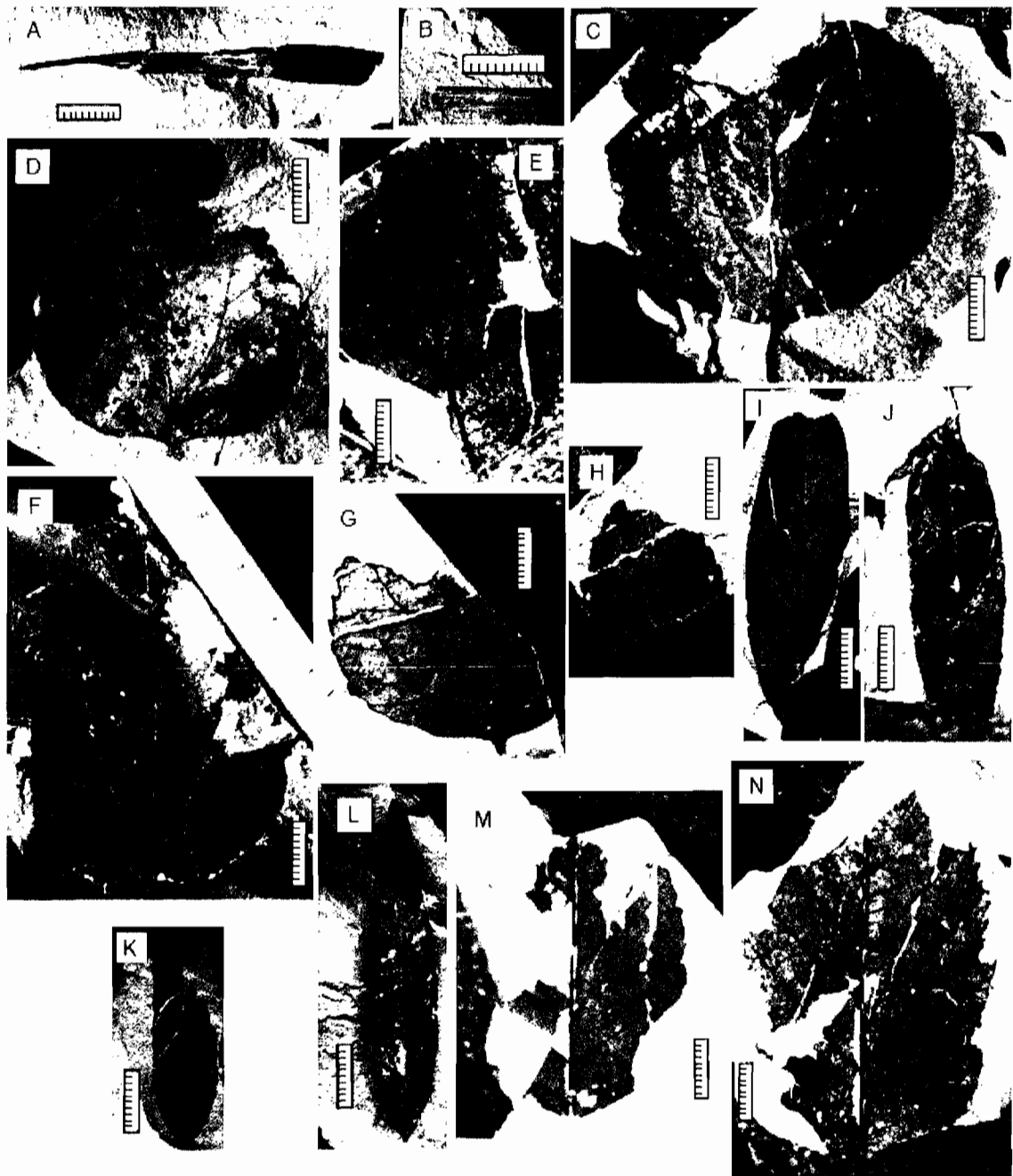
Figure 5: Cape Blanco fossils, orders Typhales, Salicales, and Fagales, scale bar is 1 cm. **A.** *Typha* sp., UO F 38108A. **B.** *Typha* sp., UO F 38110. **C.** *Populus eotremuloides*, UO F 38118A. **D.** *Populus eotremuloides*, UO F 38119A. **E.** *Populus eotremuloides*, UO F 38121. **F.** *Populus eotremuloides*, UO F 38120. **G.** *Populus lindgreni*, W 50. **H.** *Populus lindgreni* ,W 51. **I.** *Salix laevigatoides* UO F 38136A. **J.** *Salix laevigatoides* W 7. **K.** *Salix succorensis* W 29. **L.** *Salix succorensis* W 68. **M.** *Alnus harneyana* UO F 42024B. **N.** *Alnus harneyana* UO F 42025A.

relative to *P. lindgreni* may be *P. heterophylla* Linaeus, and also concur with Fields

(1996) that *P. voyana* is more like the extant aspen, *P. tremuloides*.

Family— Salicaceae

Genus—Salix

Species— *Salix laevigatoides* Axelrod

Salix coalingensis Dorf, 1930, p. 78-79; pl. 7, fig 6 only.

Salix laevigatoides Axelrod, 1950, p. 55; pl. 2, fig. 10.

Salix laevigatoides Axelrod, 1991, p. 43; pl. 8, figs. 3, 4.

Salix laevigatoides Axelrod, 1995, p 45; pl. 11, figs. 6, 7.

Referred specimens— UO F 38163A (Fig. 5I), W 7 (Fig. 5J)

Description— The diagnostic characters of *Salix* are lanceolate leaves with

semicraspedodromous to brochidodromous secondary venation and reticulate tertiary

venation. Many *Salix* species present in Miocene floras have a serrated margin. Axelrod

(1995, p. 44) provides a key to a few of the Miocene Purple Mountain species. We

follow that key and assign the entire and erose margined lanceolate *Salix* specimens from

Cape Blanco to *S. laevigatoides* with the nearest living form *Salix laevigata* Bebb of

western North America.

When originally described, Dorf (1930, pg. 78) illustrated five leaves of *S.*

coalingensis. These fossils were split by Axelrod (1944a, pg 133-134) into *Persia*

coalingensis (Dorf) Axelrod (Dorf 1930; pl. 7, fig. 7; pl. 8, figs. 1, 2), *Salix hesperia*

(Knowlton) Condit (Dorf 1930, pl . 7, fig. 6) and *Salix wildcatensis* Axelrod (Dorf 1930,

pl. 7, fig. 5). Later, Axelrod (1950, pg 55) reassigned one of Dorf's specimens (1930,

pl. 7, fig. 6) to *Salix laevigatoides* Axelrod when he established the name *Salix*

laevigatoides. No formal description was provided for the new name and therefore the

only published formal description for this species is the one by Dorf (1930). The Dorf

description applies to more material than is currently included in *Salix laevigatoides* and

so we provide a supplemental diagnosis below, relying heavily on the original description

of *Salix coalingensis* Dorf (1930) and the discussion of Axelrod (1991, pg. 43).

Supplemental Diagnosis— Leaves rather firm in texture; margin chiefly entire,

may be finely serrate; leaf narrowly lanceolate; 3.5 to 11.4 cm long; 1.2 to 2.6 cm wide;

elliptic to ovate; base cuneate to acute; apex acute to attenuate; midrib strong;

secondaries 10 to 18 pairs, thin, alternate, arising from midrib at high angle, secondary

veins brochidodromous to semicraspedodromous; tertiary veins orthogonal reticulate.

Family—Salicaceae

Genus—*Salix*

Species— *Salix succorensis* Chaney and Axelrod

Salix succorensis Chaney and Axelrod, 1959, p. 154; Pl. 16, fig. 8.

Salix succorensis Buechler et al., 2007, p. 323; Fig. 4B, G.

Referred specimens— W 29 (Fig. 5K), W 68 (Fig. 5L).

Description—The large length to width ratio, size, entire margin, and 45° angle of

secondary departure are characters unique to *Salix succorensis*. The specimens from

Cape Blanco are a very good match for the leaf figured by Buechler et al. (2007), which

has an entire margin. This echoes the comments of Fields (1996, p 411) who describes the margin as "faintly or non-toothed". However the figured specimen of Chaney and Axelrod (1959) shows teeth. The Cape Blanco specimens are entire. Modern species most closely resembling *S. succorensis* are *S. nigra* Marshall, and *S. longipes* Anderson (Chaney and Axelrod 1959), which was later reassigned to *S. caroliniana* (USDA 2009)

Order— Fagales

    Family—Betulaceae

Leaves of the Birch family have compound serrate margins and straight secondary veins. The primary obstacle to proper name assignment in the Cape Blanco specimens is the lack of complete specimens. Here we differentiate large leaves with widely spaced secondaries, and three-ordered serrate margin into *Alnus harneyana* Chaney and Axelrod and the small leaves into *Betula thor* Knowlton. The genera *Alnus* and *Betula* were distinguished by Chaney and Axelrod (1959) as follows, "(a) the leaves of Alnus are characterized by <u>strong</u> subsecondaries which diverge from the abaxial side of the secondaries in the outer part of the blade, whereas if subsecondaries are present in Betula they are only weakly developed; (b) in leaves of comparable size, *Betula* has more numerous and more closely spaced secondaries than *Alnus*; (c) in shape *Alnus* is generally wider in the lower half of the blade, not near the middle of the blade like *Betula*; (d) the marginal outline is more even in *Betula* than in *Alnus*."(page 158). Axelrod (1985, pg. 138-140) further stresses the need to consider the whole leaf to make assessments, but laments that complete Betulaceae material is rarely found. Fossil

Betulaceae have been much debated in the literature (Fields 1996, pg. 380; Axelrod 1985, pg 138; Wolfe 1966, pg. B15) although a clear review of the family has yet to be presented. Our fossils leaves are membranaceous and many are torn, indicating less resistance to transport than associated leaves.

Genus—*Alnus*

Species—*Alnus harneyana* Chaney and Axelrod

Alnus harneyana Chaney and Axelrod, 1959, p. 158-159: pl. 21, figs. 3-9

Alnus harneyana Axelrod 1985, p. 140-141; pl. 7, fig. 5

Referred specimens— UO F 42024B (Fig. 5M), UO F 42025A (Fig. 5N).

Description— A subcoriaceous to membranaceous texture, straight and uniform secondaries, and toothed margin all mark this species. The fine details of venation were preserved in the Cape Blanco specimens, but no complete leaves were recovered. Many leaf base fragments were found that match the description of Chaney and Axelrod (1959, pg. 158).

The extant species suggested by Chaney and Axelrod (1959) and Axelrod (1985) as closely resembling *Alnus harneyana* is *Alnus tenuifolia*. This name is now associated with the modern species, *Alnus incana* (L.) Moench ssp. *tenuifolia* (Nuttall) Breitung (USDA 2009) and its range is western North America. The other subspecies, *Alnus incana* (L.) Moench ssp. *rugosa* (Du Roi) R. T. Clausen, has single serrate margins and an eastern North America range. The morphological diversity observed in the sub-

species level underscores the difficulty in assigning fossils to species in the same way that we differentiate modern plants.

There is a discrepancy in the description of Chaney and Axelrod (1959, pg. 158) and modern terminology (Hickey, 1973) regarding the definition of lobed. Chaney and Axelrod (1959, pg. 158) describe *Alnus harneyana* as, "margin sinuate with the lobes mostly rounded but varying to subacute, the marginal lobes with forward-pointing serrate teeth varying from 2 to 4 (averaging 3) on lower side of lobe and usually only 1 distally." However the correct description of the marginal feature is compound serrate (following Hickey, 1973). To the original description we can add the following observations of leaf margin: toothed; serrate; with three orders convex of teeth, but teeth may have two or four orders; apical angle obtuse.

Genus—*Betula*

Species—*Betula thor* Knowlton

Betula thor Knowlton 1926, p. 35; pl. XVII, fig 3

Betula thor Chaney and Axelrod 1959, p. 160-161; pl. 23, figs. 2-6

Betula thor Wolfe 1964, p N21; pl. 1, fig. 14

Betula thor Axelrod 1985, p 141-142; pl. 23, figs. 3, 6

Betula thor Axelrod 1991, p 47-48; pl. 9, figs. 1-3, 5, 7

Betula thor Axelrod 1992, p 35-36; pl. 8, fig. 3; pl. 12, figs. 1, 2

Betula thor Axelrod 1995, p 47; pl. 14, fig. 5, pl. 15, fig. 1

Referred specimens— UO F 42027B (Fig. 6A)

Description—Small size and serrate margins characterize this species. The living plants most similar to *Betula thor* are *Betula papyrifera* Marshall and *Betula occidentalis* Hooker. Chaney and Axelrod (1959) also suggest a resemblance with *Betula nigra* Linnaeus. Combined the range of these three modern species spans North America. The modern species grow in streamside environments that are moist year round (Axelrod 1991).

Family— Fagaceae

Oak and beech leaves from Cape Blanco are diverse and distinct, without intermediate forms. In some cases two or more of the distinct forms have been included within the same fossil species as documented by Fields (1996) in his discussion of the *Quercus simulata* morphoplex.

Genus— *Chrysolepis*

Species— *Chrysolepis sonomensis* (Axelrod) Axelrod

Castanopsis sonomensis Axelrod 1944b, p. 196

Chrysolepis sonomensis Axelrod 1985, p. 144, pl. 10, figs. 1-3

Chrysolepis sonomensis Axelrod 1991, p. 49, pl. 14, figs 1, 2

Chrysolepis sonomensis Axelrod 1992, p. 37, pl. 10, figs 7, 8

Referred specimens— UO F 42054A (Fig. 6C), UO F 42053 (Fig. 6D)

Description— This entire margined, medium sized leaf with a thick midrib and clear tertiary venation is common in the Cape Blanco flora. The most similar modern species suggested by Axelrod (1985) for this fossil species is *Chrysolepis chrysophylla*

Figure 6: Cape Blanco fossils, order Fagales and Juglandales, scale bar is 1 cm. **A.** *Betula thor*, UO F 42027B. **B.** *Carya bendirei*, UO F 42029B. **C.** *Chrysolepis sonomensis*, UO F 42054A. **D.** *Chrysolepis sonomensis*, UO F 42053. **E.** *Fagus washoensis* UO F 42077A. **F.** *Fagus washoensis* UO F 42078. **G.** *Lithocarpus nevadensis* UO F 42088. **H.** *Lithocarpus nevadensis* UO F 42087. **I.** *Quercus dayana* UO F 42105A. **J.** *Quercus hannibali* UO F 42122. **K.** *Quercus hannibali* UO F 42115. **L.** *Quercus simulata* W 66. **M.** *Quercus prelobata* UO F 42138A. **N.** *Castanopsis perplexa* UO F 38056. **O.** *Quercus simulata* UO F 42142A.

(Douglas ex Hook.) Hjelmquist var. *chrysophylla* (USDA 2009) which ranges from California to Oregon and is associated with redwood forests.

Genus— *Fagus*

Species— *Fagus washoensis* LaMotte

Fagus washoensis Chaney and Axelrod, 1959, p. 164; pl. 25, figs. 7-10

Fagus idahoensis Chaney and Axelrod, 1959, p. 163; pl. 25, figs. 1-6

Referred specimens— UO F 42077A (Fig. 6E), UO F 42078 (Fig. 6F)

Description— Fields (1996) synonymized two *Fagus* species based on the existence of a continual size gradation between them, which contradicted separation of the smaller *Fagus idahoensis* by Chaney and Axelrod (1959). Most of the specimens from Cape Blanco are of the small variety, but we follow Fields (1996) for clarity. The Cape Blanco specimens are signally serrated with regular tooth spacing; apical and basal sides of the teeth convex; sinus rounded; apex simple. Secondaries diverge from primary from 30-60° and are craspedodromous straight to tooth apex. The most similar modern plant is *Fagus grandifolia* Ehrhardt.

Genus— *Lithocarpus*

Species— *Lithocarpus nevadensis* Axelrod

Lithocarpus nevadensis Axelrod, 1985, p. 145; pl. 8 figs. 8-10; pl. 24, figs. 1-7

Lithocarpus nevadensis Axelrod, 1995, p. 49; pl. 15, fig. 6

Lithocarpus nevadensis Axelrod, 1992, p. 38; pl. 9, figs. 4, 5

Referred specimens— UO F 42087 (Fig. 6H), UO F 42088 (Fig. 6G)

Description—*Lithocarpus nevadensis* was separated from similar *Quercus*
species by Axelrod (1985). The primary differences between *L. nevadensis* and *Quercus*
simulata are the spacing of the teeth, which are further apart in *L. nevadensis*, and the
shape of the secondary veins which are curved in *L. nevadensis,* and straight on *Q.*
simulata. These observations are in addition to the differences outlined by Axelrod
(1992, p 38) of *L. nevadensis* having a heavier texture and more blunt teeth. The most
similar modern species is *Lithocarpus densiflorus* (Hook. and Arn.) Rehder.

Genus— *Quercus*

Species— *Quercus dayana* Knowlton

Quercus dayana Knowlton, 1902. p. 51; pl. 6, fig. 1

Quercus dayana Chaney and Axelrod, 1959, p. 165-166; pl. 24, figs. 3-7

Referred specimens— UO F 52105A (Fig. 6I)

Description— The original description of *Quercus dayana* by Knowlton is very
apt for Cape Blanco specimens, particularly the emphasis on the thickened mid rib, weak
secondaries, entire margin, and the mesh tertiary pattern that makes individual tertiary
veins difficult to distinguish. The prominence of tertiary venation is the primary
difference between *Q. dayana* and *Q. hannibali*, with *Q. hannibali* having visible and
percurrent tertiary veins. The modern plant most similar to *Q. dayana* is *Quercus*
virginiana.

Fields (1996, pg. 342-345) suggested that *Q. dayana* of Chaney and Axelrod (1959) should be reassigned to *Chrysolepis* and is also a junior synonym of *Diospyros elliptica* Knowlton (Knowlton 1902, p. 83-84, pl. 16, fig. 5). *Diospyros elliptica* is described and figured with only four to five secondaries. This is different from the 12 or more pairs common to the leaves from Cape Blanco and the specimens listed above. The argument for placing this leaf within *Chrysolepis* is the mesh pattern of the leaf which is uncommon among the oaks. Most oak tertiary veins tend to have high relief, with exception of the modern *Q. virginiana* which resembles the Cape Blanco fossils retained in *Q. dayana*.

Genus— *Quercus*

Species— *Quercus hannibali* Dorf

Quercus hannibali Dorf, 1930, p 86; pl. 8, figs. 8-11

Quercus hannibali Chaney and Axelrod, 1959, p. 168; pl. 24, fig. 2; pl. 25, figs. 11-13

Quercus hannibali Axelrod, 1991, p 50; pl. 12, figs. 1-7

Quercus hannibali Buechler et al., 2007, p. 328; fig. 8H

Referred specimens— UO F 42122 (Fig. 6J), UO F 42115 (Fig 6K)

Description—The discussion in Chaney and Axelrod (1959, pg 166-167) of the characters of *Q. hannibali* was helpful in differentiating this species from *Q. dayana* Knowlton. In *Q. hannibali* there is a slight curve where the 2nd order veins meet the primary vein, and the 3rd order veins are usually percurrent, as they are in Cape Blanco specimens. The margin of *Q. pollardiana* can vary from entire to serrate, but the

specimens from Cape Blanco are entire. The modern plant most similar to *Q.*

hannibali is *Q. chrysolepis* Liebmann.

Genus— *Quercus*

Species— *Quercus prelobata* Condit

Quercus prelobata Condit, 1944, p. 43; pl. 7, figs. 3, 4

Quercus prelobata Chaney and Axelrod, 1959, p. 169; pl. 26, figs 8, 9; plate 27, figs 1, 2

Quercus prelobata Buechler et al., 2007, p. 332; Fig. 8A, B

Referred specimens— UO F 42138A (Fig. 6M)

Description— *Quercus prelobata* is a fossil oak that has rounded lobes. A whole

leaf was not recovered from Cape Blanco, but complete lobes were collected which

contribute to our confidence in this assignment. The size range of this species was

expanded by Buechler et al (2007) to include leaves up to 14.5 cm long. The fungal

fruiting bodies discussed by Buechler et al (2007) were not observed on the Cape Blanco

specimens. This oak has limited occurrences in Miocene floras, and it most resembles

the modern *Quercus garryana* Hooker.

Genus— *Quercus*

Species— *Quercus simulata* Knowlton

Quercus simulata Knowlton, 1898, p. 728-729; pl. 101, figs. 3, 4; pl. 102, figs. 1, 2.

Quercus simulata Chaney and Axelrod, 1959, p. 171: pl. 30, fig. 2,3,5-8; pl. 31, fig. 1-4.

Quercus simulata Buechler et al, 2007, p. 332; Fig. 8C, D.

Referred specimens— W 66 (Fig. 6L), UO F 42142A (Fig. 6O).

Description— *Quercus simulata* is a common component of Miocene floras and has been the subject of multiple taxonomic revisions and reassignments. A thorough discussion is provided by Fields (1996, pages 363-379), who develops the concept of a "*Quercus simulata* morphoplex", which is helpful in documenting convergent morphology within Fagaceae. The primary contention regarding this species results from the substantial morphological variation within the species, most notably a full transition from toothed to entire margined specimens. The Cape Blanco specimens of *Q. simulata* are toothed and have straight secondaries.

Stringently defining the morphology of the fossil, *Quercus simulata,* creates confusion when trying to identify the extant plant that is most closely resembles. Fields (1996, pg. 375) demonstrates this difficulty by presenting 17 modern species that various authors had suggested resembled *Quercus simulata*. Given this confusion we are unable to identify a closest modern relative of *Quercus simulata*.

Genus— *Castanopsis*

Species— *Castanopsis perplexa* (Knowlton) Brown

Castanopsis perplexa Brown, 1940, p. 348-349.

Castanopsis convexa Brown, 1936, p. 171; pl. 49, figs 8-11.

Referred specimens— UO F 38056 (Fig 6N).

Description— This species was reported by Brown (1936; p. 171) as resembling the modern *Castanopsis sempervirens* Dudley, which has since been revised to

Chrysolepis sempervirens (Kellogg) Hjelmqvist (USDA 2009). The fossil *Castanopsis*

perplexa was included in the *Quercus dayana* synonomy of Chaney and Axelrod (1959,

pg. 165). We disagree with this assessment because the tertiary venation in *Quercus*

dayana is a fine mesh of ~1 mm^2 areoles with secondary veins 2-3 mm apart, while in the

Cape Blanco specimens of *Castanopsis perplexa* the tertiary venation encloses a large

areola of ~4 mm^2 and lower angle, more widely spaced secondary veins. The Cape

Blanco leaves are larger than the figured examples of *Castanopsis convexa* (Brown,

1936), but are similar in size to modern *Chrysolepis sempervirens*.

Order— Juglandales

    Family— Juglandaceae

    Genus— *Carya*

    Species— *Carya bendirei* (Lesquereux) Chaney and Axelrod

Rhus bendirei Lesquereux 1888, p. 15; pl. 9, fig 2.

Carya bendirei Chaney and Axelrod, 1959, p 155; pl. 19, fig 1-5.

Carya bendirei Axelrod, 1991. p 48; pl. 11, fig 5-7.

    Referred specimens— UO F 42029B (Fig. 6B)

    Description— The original description of this species (Lesquereux 1888)

indicates that the leaf tapers toward the base, however significant variation in leaf shape

is shown by Chaney and Axelrod (1959) and Axelrod (1991). The more recently figures

fossils compare well with our specimens. The primary recognition criteria is the curved

secondary veins which diverge from the primary at a ~90° angle. Fine serration and a

transition from brochidodromous to craspedodromous are also diagnostic. The closest extant species is *Carya ovata* (Miller) Koch, a water loving species in eastern North America.

Order— Urticales

    Family— Ulmaceae

    Genus—*Ulmus*

    Species—*Ulmus speciosa*

Ulmus speciosa Newberry, 1898, p. 80; pl. 45, figs. 3, 4.

Ulmus speciosa Tanai and Wolfe 1977, p. 8; pl. 3C, F.

Ulmus speciosa Axelrod, 1991, p. 51; pl. 12, figs. 8-10; pl. 13, fig. 10.

Ulmus speciosa Meyer and Manchester, 1997, p. 82-83; pl. 18, figs. 1-6.

    Referred specimens—W 61 (Fig. 7A).

    Description— The key of Tanai and Wolfe (1977) was followed in assigning our specimens to this species, however there remains confusion about the teeth that characterize this species. In the descriptions leaves are described as doubly serrate, however in the plate both double and singular serration is documented. The tertiary venation, and asymmetrical bases observed in our specimens are identical to *Ulmus speciosa* even though the Cape Blanco specimens are overwhelmingly singly serrate. Axelrod (1991) was not satisfied with the revisions of Tanai and Wolfe (1977) regarding species level differentiation within *Ulmus*. Meyer and Manchester (1997) suggest the most similar living species is *Ulmus Americana,* but Axelrod (1991) reports it as extinct.

Genus—*Zelkova*

Species— *Zelkova browni* Tanai and Wolfe

Zelkova oregoniana Chaney and Axelrod, 1959 [part] p.174; pl.31, figs. 6, 7.

Zelkova browni Tanai and Wolfe, 1977, p. 8; pl. 4A, C-G.

Zelkova browni Buechler et al, 2007, p. 333; fig. 8I.

Referred specimens— UO F 42155 (Fig. 7D), UO F 38053 (Fig. 7F).

Description— The unique characteristic that separates *Zelkova* from *Ulmus* is alternate percurrent to regular polygonal tertiary venation (Tanai and Wolfe 1977). This character is well preserved in one of our specimens and moderate to poorly preserved in the other. The subsidiary teeth also characteristic of this species are observed in one specimen. The modern plant most similar may be *Zelkova carpinifolia,* currently restricted to Asia.

Order— Hamamelidales

Family— Platanaceae

Genus— *Platanus*

Species— *Platanus bendirei* (Lesquereux) Wolfe

Platanus dissecta Lesquereux, 1878, p. 13; pl. 7, fig. 12; pl. 10, figs. 4, 5.

Platanus dissecta Berry, 1929, p. 248; pl, 53, figs. 1, 2; pl 61.

Figure 7: Cape Blanco fossils, orders; Urticales, Hamamelidales, Ranunculales, Laurales, and Rosales, scale bar is 1 cm. **A.** *Ulmus speciosa*, W 61. **B.** *Hamamelis merriami*, UO F 42181. **C.** Angiosperm 8, UO F 42196. **D.** *Zelkova browni*, UO F 42155. **E.** *Cercocarpus nevadensis*, UO F 42208. **F.** *Zelkova browni*, UO F 38053. *Platanus bendirei*, UO F 42180. **G.** *Mahonia macginitiei*, UO F 42191. **H.** *Mahonia macginitiei*, UO F 42189. **I.** *Platanus bendirei*, W 60. **J.** *Platanus bendirei*, UO F 42172.

Platanus dissecta Chaney and Axelrod, 1959, p. 182; pl. 36, fig 3.

Platanus bendirei (Lesquereux) Wolfe, 1964, p. N24; pl 4, figs. 1, 2, 4.

Platanus bendirei (Lesquereux) Wolfe and Tanai, 1980, p. 28; pl. 3, fig. 4; pl. 4, figs. 1, 2, 4.

Referred specimens— W 60 (Fig. 7I), UO F 42172 (Fig. 7J)

Description— We follow Wolfe and Tanai (1980) in assigning our specimens to his *Platanus bendirei*. Wolfe and Tanai (1980) cite expansion of the original concept of *P. dissecta* to include both 3- and 5-lobed leaves by workers in the middle twentieth century as the reason to separate *P. bendirei* as the 3-lobed species that is more common in the Middle and Early Miocene. We do not have complete leaves from Cape Blanco, however the leaf bases that we recovered have three primary veins, indicating a three lobed leaf, and the margin clearly shows the *Platanus* axial and basal concave teeth. *Platanus bendirei* was widespread in the Miocene and all Succor Creek sycamores were assigned this name (Fields 1996). *Platanus* is commonly confused with members of *Acer*, because both families tend toward large, lobed, toothed leaves; however the large concave teeth observed in the Cape Blanco specimens are more like *Platanus*. There is no modern *Platanus* that has the marginal characteristics, lobation, and size of *Platanus bendirei*, but the characteristic shape of the *Platanus* teeth can be seen in the modern *Platanus occidentalis*.

Family— Hamamelidaceae

Genus— *Hamamelis*

Species— *Hamamelis merriami* Chaney and Axelrod

Hamamelis merriami Chaney and Axelrod, 1959, p. 180; pl. 35, figs. 1-3.

Referred specimens— UO F 42181 (Fig. 7B).

Description— This species has been identified at few localities in the Miocene, but the strong secondaries, coarsely crenate-sinuate leaves and firm texture confirm the presence of this species at Cape Blanco. The modern *Hamamelis virginiana* Linnaeus has a strong resemblance with the fossil specimens.

Order— Ranunculales

Family— Berberidaceae

Genus— *Mahonia*

Species—*Mahonia macginitiei* Axelrod

Odostemon hollicki Dorf, 1930. p. 93; pl. 10, figs. 7, 8.

Mahonia hollicki Arnold, 1936, p. 61; pl. II, figs. 3-8; pl. III, figs. 5, 7, 9.

Mahonia macginitiei Axelrod, 1985, p. 150; pl. 11, figs. 2, 4,9; pl. 27, fig. 7.

Mahonia macginitiei Axelrod, 1991, p. 52; pl. 14, figs, 3, 4, 7, 9.

Mahonia macginitiei Axelrod, 1995, p. 50; pl. 16, figs. 4, 6-9.

Mahonia macginitiei Buechler et al. 2007, p. 334; fig. 8G.

Referred specimens— UO F 42191 (Fig 7G), UO F 42189 (Fig. 7H).

Description— The secondary veins on *Mahonia* are festooned brochidodromous with the first loop occurring roughly half way between the primary vein and the margin. Tertiary veins form an irregular polygonal reticulate mesh with rectangular areoles. The

long axis of the rectangular areoles is at a high angle to the primary vein. These identifying characteristics were sufficient to determine a generic assignment for these specimens. The assignment to *Mahonia macginitiei* Axelrod is preferred over *M. simplex* (Newberry) Arnold because our specimens lack the pair of prominent basil veins that are unique to *M. simplex* (Arnold 1936, p. 61). The modern equivalent suggested by Dorf (1930, p 93) was *Odostemon aquifolium* Persh, which has been synonymized into *Mahonia aquifolium* (Persh) Nutt (USDA 2009), and this modern equivalent has been supported by subsequent authors.

Order— Laurales

    Family— Lauraceae

    Genus— *Persea*

    Species— *Persea pseudocarolinensis* Lesquereux

Persea pseudo-Carolinensis Lesquereux, 1878, p 19-20; pl. 7, figs. 1, 2.

Persea pseudocarolinensis Chaney and Axelrod, 1959, p. 177-179; pl. 34, figs. 1, 3, 4, 6.

    Referred specimens— UO P 15013 (Fig. 8A).

    Description— Long arching secondary veins are the unique identifier for this species. This species had a complicated taxonomy in the early part of the twentieth century, but we follow Chaney and Axelrod (1959) acknowledging the generalized Lauraceous appearance. The modern equivalent is likely *Persea americana* Miller, or *Persea carolinensis* Nees.

Order— Rosales

    Family— Rosaceae

    Genus— *Cercocarpus*

    Species— *Cercocarpus nevadensis* Axelrod

Cercocarpus nevadensis Axelrod, 1991, p. 51; pl. 17, figs. 6-13.

    Referred specimens— UO F 42208 (Fig 7E).

    Description— Represented by a single nearly complete specimen from Cape Blanco, the fossil *C. nevadensis* was introduced by Axelrod (1991). However, other *Cercocarpus* species are present in the Pacific Northwest, often *C. antiquus* Lesquereux, which has more closely spaced secondary veins than *C. nevadensis*. The modern species most similar to *C. nevadensis* was reported as *Cercocarpus betuloides* Nuttall by Axelrod (1991), which has since been reassigned to *Cercocarpus montanus* (USDA 2009).

    Family— Rosaceae

    Genus— *Sorbus*

    Species— *Sorbus idahoensis* Axelrod

Sorbus idahoensis Axelrod, 1985, p. 169; pl. 29, figs. 2, 6-7, 10.

    Referred specimens— W 40 (Fig. 8K).

    Description—Though based on a single specimen this leaf is unique because of its strongly single serrate margin, and narrow lanceolate shape. Higher venation details are not preserved in the Cape Blanco specimens. Axelrod (1985) suggests *Sorbus*

acuparia Linnaeus may be a modern equivalent. This may have been a typographic

error for *Sorbus aucuparia*, European Ash.

Order— Rhamnales

      Family— Rhamnaceae

      Genus— *Paliurus*

      Species— *Paliurus blakei* (Chaney) Meyer and Manchester

Ceanothus blakei Chaney, 1927, p. 128-129; pl. 16, figs. 4, 8.

Paliurus blakei Meyer and Manchester, 1997, p. 145-146; pl. 61, figs. 5, 7, 8.

      Referred specimens— UO F 42224 (Fig. 8D), UO 42216 (Fig. 8F).

      Description— Rhamnaceae are most readily identified by oblong to ovate leaves

with actinodromous primary venation. Originally described as a *Ceanothus* (Chaney

1927), Meyer and Manchester (1997) reassigned the smaller specimens with smaller teeth

to *Paliurus* and the size range includes leaves as small as those recovered from Cape

Blanco. The recovery of *Paliurus* fruits from other Oligocene localities supported the

change of name, however they acknowledge the similarity in leaves of *Paliurus* and

Ceanothus. The Cape Blanco specimens are smaller than *Ceanothus chaneyi* Dorf (Dorf

1930; page 103, pl. 13, figs 3, 4), but resemble the *Ceanothus* sp. fragment figured by

Axelrod (1944b; p. 203; pl. 38; fig. 7). The Cape Blanco specimen is differentiated from

Ceanothus edenensis Axelrod by its serrate margin. The venation and margin have a

clear resemblance to modern *Ceanothus thyrsiflorus* Eschscholtz of the California and

Oregon coast. Axelrod (1944b) suggests that a more close resemblance is seen between

Ceanothus blakei and modern *Ceanothus velutinus* Douglas however, we favor the

smaller and more prominently toothed *C. thyrsiflorus*. Since Meyer and Manchester

reassigned the genera of these specimens they suggest that the most similar modern plant

is within *Paliurus* which is currently found in southern Europe and Asia.

Order— Lamiales

    Family— Boraginaceae

    Genus— *Cordia*

    Species— *Cordia oregona* Chaney and Sanborn

Cordia oregona Chaney and Sanborn, 1933, p. 94; pl. 38, figs 4, 5.

    Referred specimens— UO F 42221A (Fig. 8C), UO F 42224 (Fig. 8G)

    Description— These leaves, subcoriaceous and well preserved at Cape Blanco,

have lengths greater than 10 cm and widths greater than 7 cm. Those figured and

described by Chaney and Sanborn (1933), had a maximum width of 4.6 cm. Despite this

discrepancy we assign the collected specimens to this name because of the similarity of

all other leaf features. Unique to *Cordia oregona* are basal secondaries parallel to the

margin for up to 1/3 of the leaf length. The modern leaf that most resembles this fossil

form is *Cordia collococca*. Images of modern herbarium specimens for *C. collacocca*

available online from the New York Botanical Garden, C. V. Starr Virtual Herbarium

(http://sciweb.nybg.org/science2/VirtualHerbarium.asp, accessed June 2, 2009).

Order— Dipsacales

    Family— Caprifoliaceae

    Genus— *Viburnum*

    Species— *Viburnum lantanafolium* Berry

Viburnum lantanafolium Berry, 1929, p 264; pl. 60, fig. 6.

Viburnum lantanafolium Chaney and Axelrod, 1959, p. 202; pl. 44, fig. 4.

    Referred specimens— UO F 42251 (Fig. 8H).

    Description— These specimens have strong third order veins that are nearly perpendicular to the primary vein. This is the character that places them in *Viburnum*. The margins of the specimens that were collected at Cape Blanco are not sufficiently preserved to conclusively say that all margin characters in the description are present, however, there is some evidence of teeth. The lack of prominent teeth precludes their assignment to *V. grahamii* (Fields 1996 p. 515). The arching character of the secondaries and their tendency to travel greater that half of the leaf length also supports their assignment to *Viburnum*. A similar modern species is *Viburnum lantana* Linné (Berry 1929).

Unknown Botanical Affiliation

    Species— Angiosperm Form 1

    Referred specimens— UO F 42253 (Fig. 8I).

Figure 8: Cape Blanco fossils, orders; Laurales, Rhamnales, Lamiales, Dipsacales, and undetermined; scale bar is 1 cm. **A.** *Persea pseudocarolinensis* P 15013. **B.** Angiosperm 9, UO F 42206. **C.** *Cordia oregona*, UO F 42221A. **D.** *Paliurus blakei*, UO F 42224. **E.** Angiosperm 2, UO F 42253. **F.** *Paliurus blakei*, UO F 42216A. **G.** *Cordia oregona*, UO F 42224. **H.** *Viburnum lantanfolium*, UO F 42251. **I.** Angiosperm 1, UO F 42253. **J.** Angiosperm 3, W 35. **K.** *Sorbus idahoensis*, W 40.

Diagnosis— Unlobed; elliptic; entire; length > 5 cm; width 1-2 cm; apex attenuate and straight; base unknown; length to width ratio > 4:1; secondary veins diverge from midrib at an angle near 90° and loop back to form semicircular area that encloses a third order mesh; tertiary veins regularly polygonal reticulate; third order veins are highest observed; tertiary vein course sinuous; areoles well developed.*Description*— The high length to width ratio and tertiary venation is suggestive of Salicaceae, but these specimen have a unique tertiary vein pattern. No whole specimen was recovered further hindering their identification. The specimen is reminiscent of *Tilia pedunculata* Chaney (Meyer and Manchester, 1997; page 111, pl. 40, fig. 6).

Species— Angiosperm Form 2

    Referred specimens— UO F 42253 (Fig. 8E).

    Diagnosis— Unlobed; elliptic; entire; length < 4 cm; width 1 cm; apex acute and straight; base acute; length to width ratio 3-4:1; brochidodromous secondary veins diverge from midrib at a moderate angle near 60°; tertiary veins alternate percurrent and sinuous; quaternary veins regular polygonal reticulate; areoles well developed.-

    Description— The small size of this leaf form is what sets it apart. The shape and venation are similar to *Quercus simulata* however there are no transitional sized leaves present and so this form is set apart. Other documented leaves of this size are *Cercocarpus* however the entire margin and acute apex show that such an assignment is incorrect.

Species— Angiosperm Form 3

Referred specimens— W 35 (Fig. 8J).

Diagnosis— Unlobed; oblong; entire; length > 3 cm; width 0.5 cm; apex acute and straight; base unknown; length to width ratio > 4:1; brochidodromous secondary veins diverge from stout midrib at high angle; third degree veins regular polygonal reticulate and sinuous; areoles well developed.

Description— Unlike Angiosperm 2, which it resembles in small size and high length to width ratio, Angiosperm 3 lacks clear quaternary venation on Angiosperm Form 3. While the size and shape of this leaf is reminiscent of *Salix churchillensis* Axelrod (1991) the venation is not similar. *S. churchillensis* secondaries loop well up into the blade and simulate a marginal vein. The secondaries on Angiosperm Form 3 are cladodromous to brochidodromous. Finer venation is not observed in *S. churchillensis* and is present on the Cape Blanco specimen, which was collected by Jack Wolfe.

Species— Angiosperm Form 4

Referred specimens— UO P 15015 (Fig. 9D).

Diagnosis— Unlobed; entire; coriaceous; elliptic; length > 5 cm, likely 8 cm; width 5 cm; apex not preserved; base rounded to straight, obtuse; length to width ratio <2:1; primary veins 3 basal actinodromous with possible marginal veins also; secondary veins brochidodromous with spacing that increases toward the base; tertiary veins alternate and sinuous; quaternary and quinternary veins regular polygonal reticulate.

Description— Basal actinodromous primary venation is limited to *Populus*, *Platanus* and *Paliurus* in the Cape Blanco Flora. However the coriaceous texture, entire margin, and lack of lobes prevent assignment to *Populus* or *Platanus*. And there is not sufficient preservation to allow assignment to the *Paliurus*. There is some resemblance in form and secondary vein shape to *Persea* however the spacing of secondaries in Angiosperm Form 4 is not consistent with *Persea*.

Species— Angiosperm Form 5

Referred specimens— UO F 42261 (Fig. 9A)

Diagnosis— Unlobed; entire at base, full margin not preserved; subcoriaceous; oblong to elliptic; length > 10 cm, likely ~12 cm; width > 3 cm, likely ~4 cm; apex not preserved; base acute to cuneate; length to width ratio 2:1 to 3:1; primary veins pinnate, secondary veins straight, depart margin at 30º, opposite, > 6 pairs, appear eucamptodromous, although margin is poorly preserved; tertiary veins not visible.

Description— The secondary veins suggest an affinity with Lauraceae or *Cornus* however without a complete margin a confident assignment is not possible.

Species— Angiosperm Form 6

Referred specimens— UO F 38054B (Fig. 9E).

Diagnosis— Degree of lobation unknown, only base was recovered; entire at base; leaf shape and size unknown, length > 5cm, width >7 cm; apex not preserved; base.

Figure 9: Cape Blanco fossils, unknown botanical affiliation, scale bar is 1 cm. **A.** Angiosperm form 5, UO F 42261. **B.** Angiosperm form 10, UO F 42207B. **C.** Angiosperm form 7, UO F 42263. **D.** Angiosperm form 4, UO P 15015. **E.** Angiosperm form 6, UO F 38054B.

rounded and obtuse; length to width ratio unknown, but likely low; primary veins, 5 palmate; tertiary veins alternate

Description— The palmate venation is unique but based on a basal fragment only. The leaf shows some resemblance to *Cercidiphyllum* and the actinodromous venation of *Acer*.

Species— Angiosperm Form 7

Referred specimens— UO F 42263 (Fig. 9C).

Diagnosis— Unlobed; entire; coriaceous; obovate; length > 10 cm, likely 14 cm; width > 6 cm; apex attenuate; base not preserved; length to width ratio ~2:1; primary veins pinnate; secondary veins diverge at a moderate angle, are brochidodromous with spacing that increases toward the base; tertiary veins percurrent and sinuous; quaternary and quinternary veins regular polygonal reticulate.

Description— These leaves resemble *Parrotia brevipetiolata* Meyer and Manchester (1997) as well as the modern *Gaultheria shallon* Pursh. The fossil record of *Gaultheria* is limited to a two specimens from the Latah flora that were originally described as *Arbutus matthesii* (Brown 1936; pg. 184-185, pl. 59, fig. 5, 6) and then later transferred to *Gaultheria pacifica* Brown (Brown 1946; pg. 351-352). The problem with assigning the Cape Blanco specimens to *Gaultheria* is the margin state which is finely serrate in the fossil and modern *Gaultheria,* but entire in the Cape Blanco specimens. The similarity of leaf morphology in Hamamelidaceae and Ericaceae highlights the difficulty in assigning proper botanical affinity to fossil specimens that lack reproductive structures. *Gaultheria* is widespread along the west coast of North America today, while extant *Parrotia* species that resemble the fossils are limited to Asia. Because of the

ambiguity in assignment and the ramifications to the floristic interpretation, we do not

assign this form to fossil species

Species— Angiosperm Form 8

    Referred specimens— UO F 42196 (Fig. 7C).

    Diagnosis—   Unlobed; entire; obovate; length > 10 cm, likely 14 cm; width > 5

cm; apex nor preserved; base not preserved; length to width ratio ~2-3:1; primary veins

pinnate; secondary veins diverge at a high angle, are brochidodromous with uniform

spacing; tertiary veins percurrent and sinuous; quaternary regular polygonal reticulate.

    Description—This large, brochidodromous, leaf is example of the mesophyll

component of the Cape Blanco flora. Assigning this specimen to a fossil species was not

possible because neither apex nor base was preserved. The high divergence angle and

uniform secondary spacing separate this form from Angiosperm 7. The wide leaf is not

within Lauraceae because the brochidodromous secondaries form tight loops close to the

margin and the secondary veins are parallel for their whole length. Large leaves within

the modern Anacardiaceae family have a strong resemblance to these fossils and are now

found in tropical regions.

    Species— Angiosperm form 9

    Referred specimens— UO F 42206 (Fig. 8B).

    Diagnosis—   Unlobed; entire; oblong; length > 10 cm, but complete leaf not

recovered; width ~ 4 cm; apex nor preserved; base acute; length to width ratio ~4-5:1;

primary veins pinnate; secondary veins diverge at a moderate to high angle, are brochidodromous with uniform spacing, secondary veins dichotomize 2/3 of the way to the margin; tertiary veins weak; thick midrib at base.

Description— This leaf is well preserved and larger than most of the Cape Blanco fossils. It has a resemblance to the modern *Rhododendron macrophyllum* D. Don ex G. Don, of western North America., and also the fossil *Magnolia lanceolata* Lesquereux, but without a complete specimen identification was not possible.

Species— Angiosperm form 10

Referred specimens— UO F 42207B (Fig. 9B).

Diagnosis— Unlobed; entire; oblong; length > 10 cm, but complete leaf not recovered; width ~ 6 cm; apex nor preserved; base acute; length to width ratio ~4-5:1; primary veins pinnate; secondary veins diverge at a moderate, are brochidodromous to cladodromous with uniform spacing; tertiary veins percurrent; quaternary venation not preserved.

Description— The gently looping secondary veins of this specimen are nearly parallel to the margin before looping into the secondary vein above them. This gives the leaves a Lauraceae appearance, but without a completely preserved specimen identification was not possible.

TAXONOMIC SUMMARY

The Cape Blanco flora is composed of at least 36 unique angiosperm leaf forms, most of them identifiable to the species level. Table 2 shows the quantities of each form, as well as the most similar extant plant, where identification was possible.

FLORISTIC INTERPRETATION

The assemblage of leaves observed in the Cape Blanco flora is a combination of forms that are well documented and commonly observed in the Miocene of the greater Oregon region (Chaney and Axelrod 1959) and few exotic, and geologically older, forms. The dominance of oaks, for example, is observed in many Miocene localities and have been used as evidence for the onset of drying and cooling climate in western North America (Axelrod, 1995). Also common in Miocene floras are the Betulaceae, Juglandaceae, and Rosaceae, which are all present at Cape Blanco. However, some of the larger leaves that were found at the Cape Blanco locality, *Cordia oregona* and Angiosperms 7, 8, and 9, are not reminiscent of leaves documented at other Miocene localities. The Cape Blanco flora is a unique Miocene assemblage with large leaved heat and water loving taxa, as well as more temperate Miocene forms.

Such tropical hold over taxa are not widely known from Miocene floras of eastern Oregon and adjacent states (e.g . Chaney and Axelrod, 1959; Fields, 1996; Beuchler et al. 2007), where paleosols, plants, and mammals are evidence of cold, dry paleoclimate and

Table 2: Fossil Quantities and Similar Modern Plants

Fossil Name	Quantity	Similar modern plant
Equisetum sp.	4	*Equisetum* sp.
Pinus tiptoniana	1	Long needle pine
Cone unit	1	Pinus? Picea?
Charcoal	14	Conifer
Needle	26	Conifer
Shredded wood	8	*Thuja? Pinus?*
Splayed needles	2	*Picea?*
Typha sp?	7	*Typha* sp?
Populus eotremuloides	20	*Populus balsamifera*
Populus lindgreni	6	*Populus heterophylia*
Salix laevigatoides	30	*Salix laevigata*
Salix succorensis	6	*Salix nigra*
Alnus harneyana	3	*Alnus tenuifolia*
Betula thor	3	*Betula papyrifera*
Chrysolepis sonomensis	46	*Chrysolepis chrysophyila*
Fagus washoensis	6	*Fagus grandifolia*
Lithocarpus nevadensis	19	*Lithocarpus densiflorus*
Quercus dayana	20	*Quercus virginiana*
Quercus hannibali	38	*Quercus chrysolepis*
Qurcus prelobata	3	*Quercus garryana*
Quercus simulata	16	?
Castanopsis perplexa	3	*Chrysolepis sepervirens*
Carya bendirei	5	*Carya ovata*
Ulmus speciosa	12	*Ulmus americana*
Zelkova browni	3	*Zelkova carpinifolia*
Platanus benderei	16	?
Hamamelis merriami	8	*Hamamelis virginiana*
Mahonia macginitiei	10	*Mahonia aquifolium*
Persea pseudocarolinensis	4	*Persea carolinensis*
Cercocarpus nevadensis	1	*Cercocarpus montanus*
Sorbus idahoensis	1	*Sorbus aucuparia*
Paliurus blakei	9	*Ceanothus thyrsiflorus*
Cordia oregona	30	*Cordia collococca*
Viburnum lantanafolium	6	*Viburnum lantana*
Angiosperm form 1	5	*Tilia?*
Angiosperm form 2	5	?
Angiosperm form 3	1	*Salix?*
Angiosperm form 4	1	?
Angiosperm form 5	2	?
Angiosperm form 6	1	*Cercidiphyllum?*
Angiosperm form 7	10	*Gaultheria?*
Angiosperm form 8	7	Anacardiaceae?
Angiosperm form 9	1	*Rhododendron?*
Angiosperm form 10	2	Lauraceae?

open grassy vegetation (Retallack 2004, 2008; Wolfe, 1994). The persistence of large

leaved species at Cape Blanco may be evidence of coastal refugia, protected from

extremes of frost and heat endured by Miocene plants of eastern Oregon. The presence

of refugia assemblages has been documented through the Tertiary in the Amazon basin of

Brazil (Hooghiemstra and van der Hammen, 1998) and their presence is used explain

modern Amazonian diversity. Similarly in Oregon, the Miocene spread of oak may not

have entirely displaced geologically older tropical species in coastal refugia.

Many of the larger leaves from Cape Blanco have prominent midribs and a

coriaceous texture, suggesting an evergreen habit as in the live oaks. Broadleaf

evergreens along with the large number of oaks suggests that the Cape Blanco flora may

represent the notophyllous broad-leaved evergreen forest of Wolfe (1979), suggesting a

mean annual temperature (MAT) between 13 º C and 20 º C. Though the presence of

conifers suggests a lower MAT, they are occasionally present in the notophyllous broad-

leaved evergreen, or 'oak-laurel' forest of Wolfe (1979).

PHYSIOGNOMIC INTERPRETATION

The basic premise of morphologically based paleoclimate analysis is that

morphological changes in modern floras can be correlated with climatic parameters. The

shape of modern leaves has been shown to correlate with temperature and precipitation

(Bailey and Sinnott, 1916; Wilf et al. 1998; Wolfe 1993). The relationships are based on

the whole composition of the flora, with the proportion of species with serrated margins

deceasing with warmer temperatures (Bailey and Sinnott, 1916) and leaf size increasing

with increase precipitation (Wilf et al. 1998). One advantage of the physiognomic method is that it is ataxonomic.

Complications arise in the morphological descriptions because there is not a documented theoretical understanding of why leaves are shaped the way they are. Such data would inform the collection of morphological features. The characters considered important by Wolfe (1993), are shown for each species, including unassigned forms, in Table 3. Morphological description was based on material collected from Cape Blanco, and published descriptions. These data emphasize overall leaf shape and margin character without addressing venation patterns. However, the venation patterns are essential in name assignment and the establishment of the unnamed angiosperm forms.

Two specific techniques of physiognomic interpretation are multivariate analysis of a suite of leaf morphologic characters are associated with many climate parameters (Wolfe 1993), and univariate analysis of a single morphological feature correlated with a single measured climate variable. Both methods have advantages and disadvantages, the multivariate method can yield more data, yet suffers from lack of transparency, variables that co-vary, and difficulty in defining the error of results. The univariate method is straight forward and transparent, but perhaps does not extract the full measure of data from the flora. Both methods suffer from a lack of theoretical underpinning and thus solely rely on empirical observations. Here we apply the two most robust univariate analysis, those that estimate mean annual temperature and mean annual precipitation, to the Cape Blanco Flora.

There are 36 unique angiosperm forms in the Cape Blanco flora, 34 of them have a single margin state, and 55.5% of the single margin state species or species equivalents are entire. Using the equation of Wing and Greenwood (1993) LMAT = 30.6P + 1.14, where LMAT is leaf estimated mean annual temperature, and P is the proportion of species that have entire margins , the LMAT of the Cape Blanco Flora is, 18.24 ° C ± 2.6 ° C, the error is calculated following Wilf (1997). This result corresponds well with the floristically derived MAT estimate. The current mean annual temperature at Cape Blanco is ~11 ° C (Wolfe 1993).

The paleoprecipitation at Cape Blanco can be estimated in a similar fashion. Following the equations of Wilf et al.(1998), the mean annual precipitation at Cape Blanco is 201 cm (+ 86 cm, -61 cm). This is slightly more than the195 cm per observed today at Cape Blanco year (Wolfe 1993).

PALEOTOPOGRPAHY

Paleoelevation of the Cape Blanco flora is based on the sedimentological evidence of sea level deposition. Comparable modern species are evidence that both streamside and hill-slope vegetation types were present. This supports the sedimentological evidence for disturbance of an entire local catchment area by volcanic ash fall.

Table 3: Morphology of Leaves (a)

Species	Form	Teeth					Leaf Size								
	Lobed	None	Regular	Close	Round	Acute	Cmpd.	Nano.	Lepto. 1	Lepto. 2	Micro. 1	Micro. 2	Micro. 3	Meso. 1	Meso. 2	Meso. 3
Populus eofremontides	0	0.5	0.25	0.25	0.25	0.5	0	0	0	0	0	0.33	0.33	0.33	0	0
Populus imagrew	0	0	1	0.5	0.5	0.25	0	0	0	0	0	0.33	0.33	0.33	0	0
Salix laevigatoides	0	0.5	0.25	0.25	0	0.5	0	0	0	0	0.5	0.5	0	0	0	0
Salix susocarensis	0	1	0	0	0		0	0	0	0	0.5	0.5	0	0	0	0
Alnus harneyana	0	0	1	0.5	0.5	0.5	1	0	0	0	0	0	0.5	0.5	0	0
Betula thor	0	0	1	0.5	0.5	0.5	1	0	0	0	0	0.5	0.5	0	0	0
Chrysolepis sonomensis	0	1	0	0	0	0	0	0	0	0	0	0.5	0.5	0	0	0
Fagus washoensis	0	0	1	1	0	1	0	0	0	0	0	1	0	0	0	0
Lithocarpus nevadensis	0	0	0.5	0.5	0.5	0.5	0	0	0	0	0	0.5	0.5	0	0	0
Quercus dayana	0	1	0	0	0	0	0	0	0	0	0.33	0.33	0.33	0	0	0
Quercus hannibali	0	1	0	0	0	0	0	0	0	0	0	0.5	0.5	0	0	0
Quercus prelobata	1	1	0	0	0	0	0	0	0	0	0	1	0	0	0	0
Quercus simulata	0	0	1	1	1	0	0	0	0	0	0	0.5	0.5	0	0	0
Castanopsis perplexa	0	1	0	0	0	0	0	0	0	0	0	0	0.5	0.5	0	0
Carya bendirei	0	0	1	1	0	1	0	0	0	0	0	0.5	0.5	0	0	0
Ulmus speciosa	0	0	1	1	0.5	0.5	0	0	0	0	0	0.5	0.5	0	0	0
Zelkova browni	0	0	1	1	0.5	0.5	0	0	0	0	0	0.5	0.5	0	0	0
Platanus bendirei	1	0	1	1	0	1	0	0	0	0	0	0	0.5	0.5	0	0
Hamamelis merriami	0	0	1	0	1	0	0	0	0	0	0	0	0.5	0.5	0	0
Mahonia macginitiei	0	1	0	0	0	0	0	0	0	0	0	0.5	0	0	0	0
Persea pseudocarolinensis	0	1	0	0	0	0	0	0	0	0	0	0	0.5	0.5	0	0
Cercocarpus revolutonsis	0	0	1	1	0	1	0	0	0	0	0	1	0	0	0	0
Sorbus washoensis	0	0	1	1	0	1	0	0	0	0	1	0	0	0	0	0
Paliurus blackei	0	0	1	1	0.5	0.5	0	0	0	0	0.5	0.5	0	0	0	0
Cordia oregona	0	1	0	0	0	0	0	0	0	0	0	0	0.5	0.5	0	0
Viburnum lantanafolium	0	0	1	1	0	1	0	0	0	0	0	0	0	1	0	0
Angiosperm form 1	0	1	0	0	0	0	0	0	0	0	0	0.5	0.5	0	0	0
Angiosperm form 2	0	1	0	0	0	0	0	0	0	0	1	0	0	0	0	0
Angiosperm form 3	0	1	0	0	0	0	0	0	0	0	1	0	0	0	0	0
Angiosperm form 4	0	1	0	0	0	0	0	0	0	0	0	0.5	0.5	0	0	0
Angiosperm form 5	0	1	0	0	0	0	0	0	0	0	0	0	0.5	0.5	0	0
Angiosperm form 6	?	1	0	0	0	0	0	?	?	?	?	?	?	?	?	?
Angiosperm form 7	0	1	0	0	0	0	0	0	0	0	0	0	0.5	0.5	0	0
Angiosperm form 8	0	1	0	0	0	0	0	0	0	0	0	0	0	1	0	0
Angiosperm form 9	0	1	0	0	0	0	0	0	0	0	0	0	0	1	0	0
Angiosperm form 10	0	1	0	0	0	0	0	?	?	?	?	?	?	?	?	?

(a) Morphology of fossil leaves with categories following Wolfe (1993). Abbreviations: Cmpd. compound; Nano. nanophyll; Micro. microphyll; Meso. mesophyll; Atten. attenuate.

TAPHONOMY

Most fossils recovered from Cape Blanco were fragmentary. The leaf fragments had clean edges due to mechanical processes during transport rather than biologic decay. Leaf size, density, and chemical composition can affect the quantity of leaves entering the sediment supply system as well as how the leaves are transported (Ferguson, 1985). The fossil leaves collected from Cape Blanco had a range of size and shapes suggesting that no systematic exclusion of forms occurred. Further, our analysis is based on presence or absence of forms and not quantities. which decreases the sensitivity to taphonomic bias.

CONCLUSION

The Cape Blanco flora records a warm, wet, and diverse forest on the western coast of North America in the early Miocene. The presence of geologically older, thermophilic taxa, as well as geologically younger temperate taxa may indicate that the coast served as a refugia. The temperature indicated by the leaves is much warmer than observed today, however the precipitation level is similar. This is good evidence that the atmospheric and ocean patterns that drive precipitation in the region today were well developed in the early Miocene, but that precipitation was likely derived from an ocean with much warmer surface temperatures than are observed today.

The following chapter explores the implications of the mean annual temperature estimate presented in this chapter and compares it to oxygen isotope based temperature estimates.

CHAPTER IV

EARLY MIOCENE TEMPERATURE GRADIENTS, A COMPARISON OF

PALEOBOTANICAL AND ISOTOPIC PREDICTIONS

Introduction:

Miocene time may be a climate analogue for future global change. Modeling of

the ongoing greenhouse warming (Solomon et al., 2007) predicts atmospheric CO_2 levels

of ~ 500 ppm by the year 2100. This is comparable with the early and middle Miocene

atmospheric CO_2 inferred from stomatal indices of fossil leaves (Kürschner et al., 2008).

Carbon dioxide and temperature are well correlated in the modern and many different

records suggest that the Miocene was warmer than today (e.g., Böhme 2003, Cosgrove et

al. 2002, Zachos et al. 2001). But, these studies provide only relative results; mean

annual temperature in °C, is not provided, and absolute results are necessary to

quantitatively compare different methods and calibrate general circulation models. The

late Early Miocene is an ideal time to analyze climate because it is between the Mi-1

Glaciation and Mid-Miocene Climatic Optimum (Zachos et al. 2001), when the global

$\delta^{18}O$ record is relatively stable. This suggests that the climate variation of the late Early

Miocene was more constrained than during times of great climate fluctuations. Absolute

paleotemperature estimates from the Early Miocene may therefore serve as a guide for the magnitude and distribution of global heat when Earth's atmosphere contains more CO_2.

Recognition of generally warmer conditions during the Miocene allows for new hypotheses regarding how this additional heat is distributed globally. Two methods that estimate past surface air temperature are leaf margin analysis of fossil floras (Wolfe 1979) and sea surface temperature estimates from planktonic and benthic foraminifers (Zachos et al. 1994). Here I address three important questions. First, is there agreement between the two methods that yield Early Miocene absolute air temperature? Second, are the latitudinal temperature gradients for the Early Miocene the same between the two methods? Finally, are the Miocene gradients the same as Holocene and modern latitudinal temperature gradients?

Methods:

Paleobotanical:

Bailey and Sinnott (1916) recognized that the portion of woody dicot plants with smooth (entire) margined leaves increases with temperature. The relationship is robust and documented globally (Wolfe 1979, Gregory-Wodzicki 2001, Greenwood et al. 2004). A least squares linear regression of leaf margin state and mean annual temperature allows for estimates of ancient mean annual temperature (Wing and Greenwood, 1993; Wilf, 1997). Here I estimate the leaf mean annual temperature (LMAT) for three late Early

Miocene floras from the west coast of North America: the ~18 Ma, Temblor (Renney 1972), Cape Blanco (Chapter three, this volume), and Seldovia (Wolfe and Tanai, 1980) floras (Figure 1). Coastal floras are ideal to compare with sea surface temperatures because their interpretation is not complicated by paleoaltitude or rain shadow effects.

The Temblor Flora was recovered from the Temblor formation at a locality 9 miles north of Coalinga, California, USA (Renney 1972) which Renney (1972) regarded as middle Miocene and ~15.5 Ma. The stratigraphy of the region has since been revised and based on lithology, the plant fossil beds described by Renney (1972) correlate with the estuarine facies tract of Bridges and Castle (2003). This updates the age of the fossil flora to 17.5 ± 1 Ma based on regional bounding surfaces and their correlation to the global sea level curve of Haq et al. (1987). The estuarine facies tract is the second of five facies tracts that range from incised valley to subtidal.

The Cape Blanco flora was recovered from the sandstone of Floras Lake at a locality southeast of Cape Blanco, OR (Chapters 2 and 3 this volume). The ^{40}Ar-^{39}Ar age of the flora is 18. 26 ± 0.86 Ma and it was deposited at sea level. It is a mixed oak laurel forest with streamside as well as hill slope vegetation.

The Seldovia Point flora (Wolfe and Tanai, 1980) was recovered from multiple localities within the late Early Miocene Tyonek Formation (Calderwood and Fackler, 1972), in the Kenai Peninsula, Alaska. Based on stratigraphic position and correlation, the age of the formation is late Early Miocene to early Middle Miocene (16 to 18 Ma), and the floras were deposited in a slow moving fluvial system. Low gradient fluvial
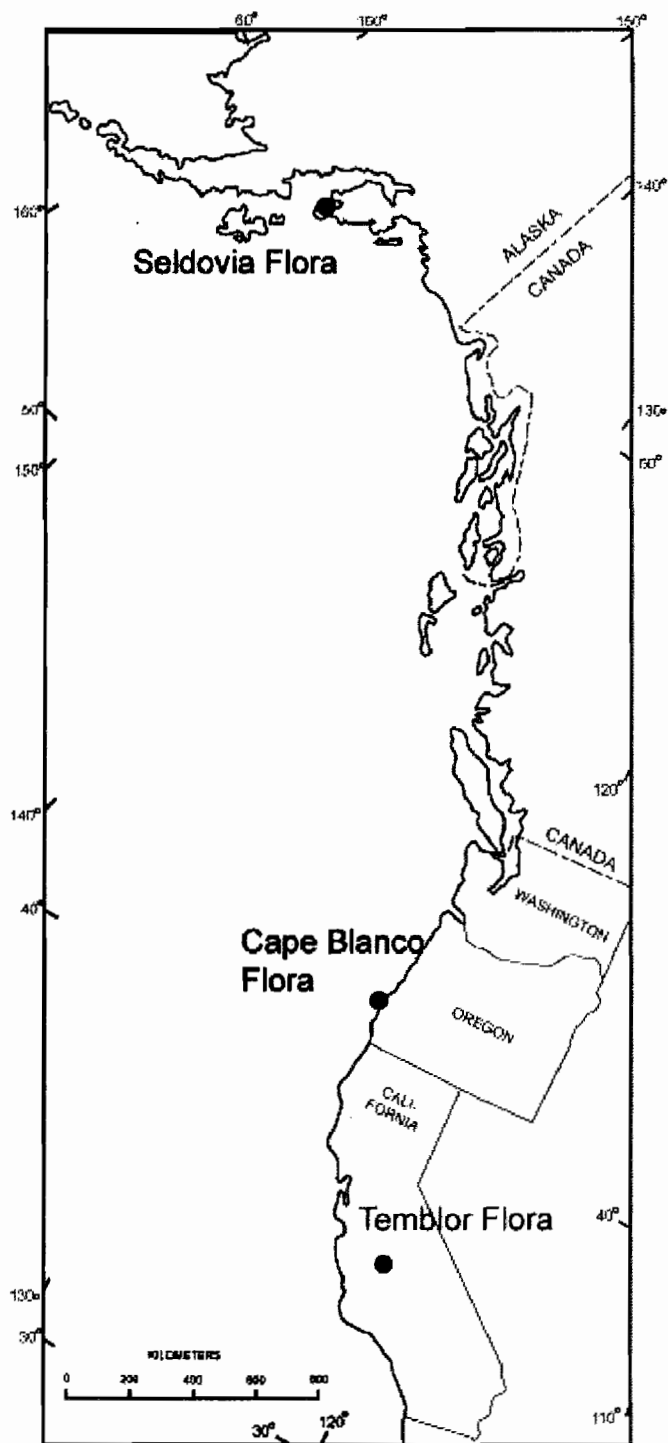
Figure 1: Map of Flora Locations

deposition along with the formation thickness, areal extent, and duration of deposition, all suggest that the unit was deposited near sea-level (Wolfe and Tanai 1980).

The margin type for fossil plant species from the Temblor and Cape Blanco floras was recorded, and the percent of entire margins was calculated. The determination of character state was from figures and descriptions of Renny (1972) and Emerson (this Dissertation). Wolfe and Tanai (1980) reported the percentage of entire species for the Seldovia Point flora. Based on the number of entire leaves, leaf mean annual temperature (LMAT of Wing and Greenwood, 1993) was calculated (Table 1).

Table 1: Climate data estimated from fossil floras[a]

	Temblor	Cape Blanco	Seldovia
Lat.	36	43	59
Total Forms	31	34	54
Percent Entire	21	19	9
LMAT	21.8	18.2	6.2
error	2.6	2.6	1.5

[a] Latitude is in degrees N. 'Total Forms' is the number of unique leaf types that had a single margin state. 'Percent entire' is the number of forms that had a smooth margin. 'LMAT' is calculated using the equation of Wing and Greenwood (1993) $LMAT = 30.6P + 1.14$, where LMAT is leaf estimated mean annual temperature, and P is the proportion of species that have entire margins. 'Error' is one standard deviation and is calculated following Wilf (1997, eq. 4).

Geochemical:

The early Middle Miocene (15.5 to 16.5 Ma, N-8) benthic foraminifera compilation (n=83) of Savin et al. (1985) was used to estimate late Early Miocene sea surface temperature (SST). To follow the calcite/water $\delta^{18}O$ temperature equation of Erez and Luz (1983), it was necessary to estimate the isotopic composition of the early Miocene ocean at the sample latitudes ocean by using equation one of Zachos et al.

(1994) and adding a -0.5 ‰ ice volume correction. Zachos et al. (1994) used the same ice volume correction value for their early Oligocene study. The SST estimates are the circle symbols on the plot of absolute latitude verses temperature (Figure 2). The entire global dataset is used because the northeastern Pacific region Miocene has been little sampled by deep sea drilling (e.g., Woodruff and Savin, 1989). The Holocene temperature measurements also used data compiled by Savin et al. (1985) and followed the same method of SST estimation, however no ice volume correction was used.

Modern Observed Temperatures:

Modern weather station data for the west coast of North America (Bryson and Hare, 1974) and South America (Schwerdtfeger, 1976) are also plotted on Figure 2.
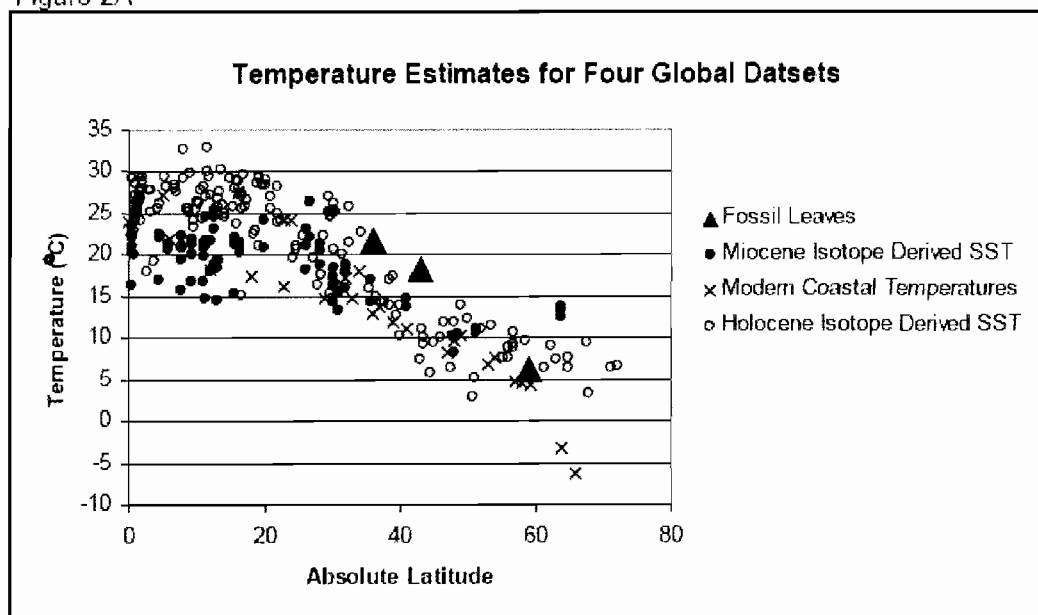
Analysis:

The four global data sets are plotted with absolute latitude on the x-axis and temperature ($^\circ$ C) on the y axis, Figure 2A. A subset of the global data sets was also analyzed. The northern hemisphere, temperate latitude (23.3 $^\circ$ N to 66.6 $^\circ$ N), portions of the data sets, and their least squares linear regressions are shown in Figures 2B and 2C.

Results:

Linear regressions of the four global data sets showed no coincident slopes, and student t-test confirmed with greater than 99.9% confidence that the slopes were unique.

Figure 2A

Temperature Estimates for Four Global Datsets

Legend:
▲ Fossil Leaves
● Miocene Isotope Derived SST
× Modern Coastal Temperatures
○ Holocene Isotope Derived SST

Temperature Estimates for Northern Hemispere Temperate Global Datsets

Figure 2B

Fossil leaves and Modern Coastal Temperatures

$y = -0.6906x + 47.17$
$R^2 = 0.9937$

$y = -0.618x + 38.69$
$R^2 = 0.9535$

Figure 2C

Isotope Derived Sea Surface Temperatures

$y = -0.2642x + 29.031$
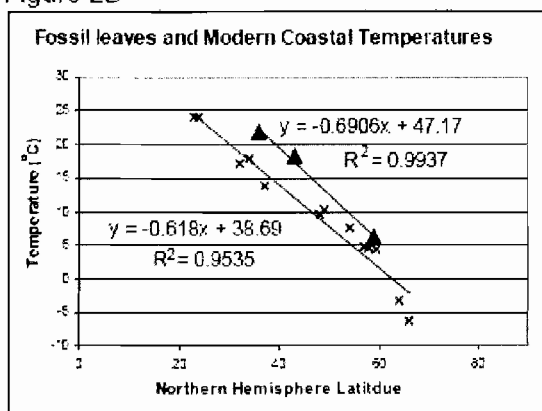$R^2 = 0.6893$
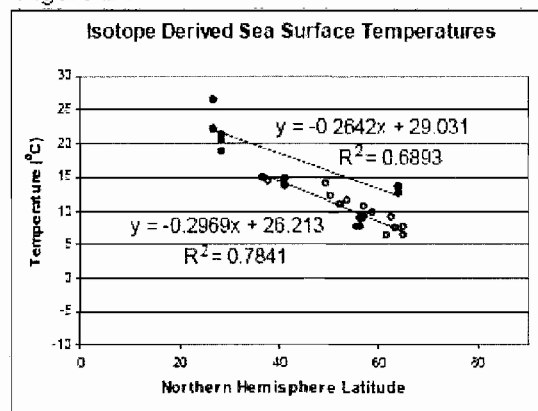
$y = -0.2969x + 26.213$
$R^2 = 0.7841$

Figure 2: Temperature data. A; all global data plotted with absolute value of latitude, B; Northern Hemisphere Temperate fossil leaf data and modern temperature station measurements with linear regressions of the two data sets, C; Northern Hemisphere temperate sea surface estimates with linear regressions of the two data sets.

The northern hemisphere temperate latitude subset, however, is more interesting. The fossil leaf slope and the modern temperature slope could not be differentiated with greater than 95% confidence. The Miocene and Holocene isotope slopes could not be differentiated from each other with greater than 90% confidence, but they were different than the modern and leaf slopes. The off-sets of the slope coincident regressions are 5.2 °C for the leaf versus modern and 4.2 °C for the Miocene versus Holocene isotopes as measured at 45 °N. In both cases the Miocene measurements are warmer.

Discussion:

The global data set when considered from an absolute latitude perspective fails to yield compelling results, probably because the northern and southern hemispheres have fundamentally different land and ocean distributions. Furthermore, to accurately model the temperature gradient from equator to pole data should be evenly distributed among the latitudes and this is not the case with the isotopic and leaf data sets.

The most robust result of this study is that the offset between the Miocene leaf and modern regressions (5.2 °C) and the Miocene isotope and Holocene isotope regressions (4.2 °C) which are within one degree Celsius. This magnitude of temperate increase matches the temperature increase predicted for 2100 (Solomon et al. 2007).

The coincident slopes of the two data sets are also of note. That the fossil leaf and modern weather station data have the same latitudinal gradient ~ -0.6 ° C/degree latitude suggests that fossil leaves are an accurate climate predictor. The coincident slopes for the isotope data suggest that the equations used to convert measured $\delta^{18}O$ to SST in °C may

have a large control of the °C results and/or the Miocene and Holocene oceans had the same latitudinal temperature gradient.

But, which gradient is correct, the isotopes or the fossil? It is likely that they both are. The ocean temperature is moderated both by the high heat capacity of water and ocean currents. The air has a lower heat capacity and so its temperature is more sensitive to energy differences at the equator and pole. This discrepancy may explain why the land based measurements have a steeper latitudinal temperature gradient. The coincident offset in the temperatures between the oceans and land is likely due to the climate buffering capacity of CO_2 which increased the heat capacity of the atmosphere and can, through atmospheric circulation, transfer heat between the oceans and continents resulting in a similar overall temperature increase.

The recognition of shallower gradients in the isotope data calls for caution when using these data to predict polar and tropical land temperatures, as the may be over and under predicted, respectively. The possibility of warmer low latitudes challenges models where the global heat budget is predominantly accommodated by an increase in high latitude temperature (Crowley and Zachos 2000; Nikolaev et al. 1998).

The Miocene remains an important time for understanding global climate change because tectonic arrangements during Miocene time were similar to today (Herold et al. 2008), however two major changes with the potential to drastically change ocean circulation, the closure of the Panamanian isthmus (Duque-Caro 1990), and the opening of the Bering Strait (Marincovich and Gladenkov 1999), preclude direct comparisons.

Promising modeling results (Motoi et al. 2005) have begun to address and quantify the results of ocean circulation differences between the early Miocene and today.

Conclusion:

Both paleobotanical and oxygen isotope methods estimate that the Late Early Miocene in the northern hemisphere was ~5°C warmer than today. This magnitude increase is the same as models predict occurring by 2100 (Solomon et al. 2007). The predicted atmospheric CO_2 in 2100 is also the same as is estimated for the late Early Miocene, ~ 500 ppm. The global data set was inconclusive and the temperate northern hemisphere had to be considered independently for compelling results to be obtained. The latitudinal gradients predicted by fossil leaf measurements did not match those from the sea. This may be because of systematic error within the methods, or actual differences in temperature of the ocean and the land.

CHAPTER V

CONCLUSIONS

Together, the three data chapters of this dissertation document the Cape Blanco

flora and its paleoclimatic significance. Chapter two shows that 18.26 ± 0.86 Ma during

normal polarity chron C5En a rhyodacitic eruption in the Western Cascades blanketed the

Klamath terrain with pumice and ash, which overwhelmed a catchment leading to a local

progradation. Leaves of the trees growing at that time were carried along wit the ash and

deposited in a lagoon near the shore. In the third chapter I apply names to the recovered

fossils and document their diversity. Based on the size and margin state of the leaves I

estimate a mean annual temperature of ~18 ° C and a mean annual precipitation of ~200

cm/yr for the Cape Blanco flora. The fourth chapter compares the Cape Blanco

paleotemperature results along with paleotemperature estimates from the Temblor flora

of California and the Seldovia flora from Alaska to paleotemperatures estimated from

oxygen isotopic analysis of benthic foraminifera. The leaf data estimate a latitudinal

gradient of ~ 0.7 ° C/degree latitude, and the isotopic predicted gradient is ~0.27 °

C/degree latitude. Both results agree that the mean annual temperature at 45 ° C was 4-5

° C warmer than today in the late early Miocene.

REFERENCES

Aalto, K. R., 2006, The Klamath peneplain: A review of J.S. Diller's classic erosion surface, *in* Snoke, A. W., and Barnes, C. G., eds., Geological studies in the Klamath Mountains province, California and Oregon. A volume in honor of William P. Irwin: Boulder, Colorado, The Geological Society of America, p. 451-464.

Addicott, W. O., 1976, Neogene molluscan stages of Oregon and Washington, *in* Fritsche, A. E., Ter Best, H. J., and Wornardt, W. W., eds., The Neogene Symposium. San Francisco, Society of Economic Paleontologists and Mineralogists, Pacific Section, p. 95-115.

Addicott, W. O., 1980, Miocene stratigraphy and fossils, Cape Blanco, OR. Oregon Geology, v. 42, no. 5, p. 87-98.

Addicott, W. O., 1983, Biostratigraphy of the Marine Neogene Sequence at Cape Blanco, Southwestern Oregon. Geological Survey Professional Paper 774-G Shorter Contributions to General Geology, p. G1-G19.

Albright L. B., III, Woodburne, M. O., Fremd, T. J., Swisher, C. C. I., MacFadden, B. J., and Scott, G. R., 2008, Revised Chronostratigraphy and Biostratigraphy of the John Day Formation (Turtle Cove and Kimberly Members), Oregon, with Implications for Updated Calibration of the Arikareean North American Land Mammal Age. The Journal of Geology, v. 116, p. 211-237.

Allison, R. C., and Addioctt, W. O., 1976, The North pacific Miocene Record of *Mytilus (Plicatomytilus)*, a New Subgenus of Bivalvia. Geological Survey Professional Paper 962, p. 21, 3 pl.

Armentrout, J. M., 1980, Cenozoic Stratigraphy of Coos Bay and Cape Blanco, Southwestern Oregon, *in* Oles, K. F., Johnson, J. G., Niem, A. R., and Niem, W. A., eds., Geologic Field Trips in Western Oregon and Southwestern Washington. Portland, Oregon, State of Oregon Department of Geology and Mineral Industries, Bulletin 101, p. 175-216.

Armentrout, J. M., Hull, D. A., Beaulieu, J. D., and Rau, W. W., 1983, Correlation of Cenozoic Stratigraphic Units of Western Oregon and Washington. State of Oregon Department of Geology and Mineral Industries, Oil and Gas Investigation 7, 87 p., 1 chart.

Arnold, C. A., 1936, Some fossil species of *Mahonia* from the Tertiary of Eastern and Southeastern Oregon. Contributions from the Museum of Paleontology, The University of Michigan, v. 5, no. 4, p. 55-66 (3 pls.).

Ashwill, M., 1983, seven fossil floras in the rain shadow of the Cascade Mountains, Oregon. Oregon Geology, v. 45, p. 107-111.

Axelrod, D. I., 1944a, The Mulholland Flora, *in* Chaney, R. W., ed., Pliocene Floras of California and Oregon. Washington, D. C., Carnegie Institution of Washington, Publication 553, p. 103-128.

Axelrod, D. I., 1944b, The Sonoma Flora, *in* Chaney, R. W., ed., Pliocene Floras of California and Oregon. Washington, D. C., Carnegie Institution of Washington, Publication 553, p. 167-206.

Axelrod, D. I., 1950, A Sonoma Florule from Napa, California, *in* Axelrod, D. I., ed., Studies in Late Tertiary Paleobotany. Washington, D. C., Carnegie Institution of Washington Publication 590, p. 23-71.

Axelrod, D.I., 1964, The Miocene Trapper Creek Flora of Southern Idaho. Berkeley, CA, University of California Press, 148 p

Axelrod, D. I., 1968, Tertiary Floras and Topographic History of the Snake River Basin, Idaho. Geological Society of America Bulletin, v. 79, p. 713-734.

Axelrod, D. I., 1985, Miocene Floras from the Middlegate Basin, West-Central Nevada. Berkeley, University of California Press, 209 p.

Axelrod, D. I., 1991, The Early Miocene Buffalo Canyon Flora of Western Nevada. Berkeley, University of California Press, 76 p.

Axelrod, D. I., 1992, The Middle Miocene Pyramid flora of Western Nevada. Berkeley, University of California Press, 50 p.

Axelrod, D. I., 1995, The Miocene Purple Mountain Flora of Western Nevada. Berkeley, University of California Press, 62 p.

Bailey, I. W., and Sinnott, E. W., 1916, The Climatic Distribution of Certain Types of Angiosperm Leaves. American Journal of Botany, v. 3, no. 1, p. 24-39.

Baldwin, E. M., 1945, Some revisions of the late Cenozoic stratigraphy of the Southern Oregon Coast. Journal of Geology, v. 53, no. 1, p. 35-46.

Bandy, O. L., 1950, Some later Cenozoic Foraminifera from Cape Blanco, Oregon. Journal of Paleontology, v. 24, no. 3, p. 269-281.

Beck, M. E. J., and Plumley, P. W., 1980, Paleomagnetism of intrusive rocks in the Coast Range of Oregon. Microplate rotations in middle Tertiary time. Geology, v. 8, p. 573-577.

Berry, E. W., 1929, A Revision of the Flora of the Latah Formation; U.S. Geological Survey Professional paper 154-H, Shorter contributions to general geology, 1928. Washington, DC, United States Government Printing Office.

Bockheim, J. G., Kelsey, H. M., and Marshall III, J. G., 1992, Soil Development, Relative Dating, and Correlation of Late Quaternary Marine Terraces in Southwestern Oregon. Quaternary Research, v. 37, p. 60-74.

Bockheim, J. G., Marshall, J. G., and Kelsey, H. M., 1996, Soil-forming processes and rates on uplifted marine terraces in southwestern Oregon, USA. Geoderma, v. 73, p. 39-62.

Böhme, M., 2003, The Miocene Climatic Optimum: evidence from ectothermic vertebrates of Central Europe. Palaeogeography, Palaeoclimatology, Palaeoecology, v. 195, p. 389-401.

du Bray, E. A., John, D. A., Sherrod, D. R., Evarts, R. C., Conrey, R. M., and Lexa, J., 2006, Geochemical Database for Volcanic Rocks of the Western Cascades, Washington, Oregon, and California, U.S. Geological Survey Data Series 155, 49 p.

Bridges, R. A., and Castle, J. W., 2003, Local and regional tectonic control on sedimentology and stratigraphy in a strike-slip basin: Miocene Temblor Formation of the Coalinga area, California, USA. Sedimentary Geology, v. 158, p. 271-297.

Brown, R. W., 1936, Additions to some fossil floras of the western United States, U.S.G.S. Professional Paper 186-J. Washington, DC, Department of the Interior.

Brown, R. W., 1940, new species and changes of name in some American fossil floras. Journal of the Washington Academy of Sciences, v. 30, no. 8, p. 344-356.

Brown, R. W., 1946, Alterations in some fossil and living floras. Journal of the Washington Academy of Sciences, v. 36, no. 10, p. 344-355.

Bryson, R. A., and Hare, F. K., 1974, Climates of North America. Amsterdam-London-New York, Elsevier Scientific Publishing Company, p. 420.

Buechler, W. K., Dunn, M. T., and Rember, W. C., 2007, Late Miocene Pickett Creek Flora of Owyhee County, Idaho. Contributions from the Museum of Paleontology, The University of Michigan, v. 31, no. 12, p. 305-362.

Calderwood, K. W., and Fackler, W. C., 1972, Proposed Stratigraphic Nomenclature for Kenai Group, Cook Inlet Basin, Alaska. The American Association of Petroleum Geologists Bulletin, v. 56, no. 4, p. 739-754.

Cas, R. A. F., and Wright, J. V., 1987, Volcanic Successions Modern and Ancient. London, Allen & Unwin, 528 p.

Chaney, R. W., 1927, Geology and Palaeontology of the Crooked River Basin, with special reference to the Bridge Creek Flora. Washington D.C., Carnegie Institution of Washington: Publication No. 346, p. 45-138.

Chaney, R.W., 1938, The Deschutes Flora of Eastern Oregon, Miocene and Pliocene Floras of Western North America. Washington D.C., Carnegie Institution of Washington: Publication No. 476, p. 185-216

Chaney, R. W., and Axelrod, D. I., 1959, Miocene Floras of the Columbia Plateau. Washington, D.C., Carnegie Institution of Washington, 237 p.

Chaney, R. W., and Sanborn, E. I., 1933, The Goshen Flora of West Central Oregon. Washington, Carnegie Institution of Washington Publication Number 439, 103 p.

Chaney, R.W., Condit, C., and Axelrod, D.I., 1944, Pliocene Floras of California and Oregon. Washington D.C., Carnegie Institutions of Washington, Publication 553, 407 p.

Christiansen, R. L., and Yeats, R. S., 1992, Post-Laramide geology of the U.S. Cordilleran region, *in* Burchfiel, B. C., Lipman, P. W., and Zoback, M. L., eds., The Cordilleran Orogen. Conterminous U. S.. Boulder, Colorado, Geological Society of America, The Geology of North America, v. G-3, p. 261-406.

Clifton, H. E., Hunter, R. E., and Phillips, L. R., 1971, Depositional Structures and processes in the non-barred high-energy nearshore. Journal of Sedimentary Petrology, v. 41, no. 3, p. 651-670.

Condit, C., 1944, The Remington Hill Flora, *in* Chaney, R. W., ed., Pliocene Floras of California and Oregon. Washington D.C., Carnegie Institution of Washington, p. 21-39.

Cosgrove, B. A., Barron, E. J., and Pollard, D., 2002, A simple interactive vegetation model coupled to the GENESIS GCM. Global and Planetary Change, v. 32, p. 253-278.

Crowley, T. J., and Zachos, J. C., 2000, Comparisons of zonal temperature profiles for past warm time periods, *in* Huber, B. T., Macleod, K. G., and Wing, S. L., eds., Warm Climates in Earth History. Cambridge, Cambridge University Press, p. 50-76.

Diehl, J. F., Beck, M. E. J., Beske-Diehl, S., Jacobson, D., and Hearn, B. C. J., 1983, Paleomagnetism of the late Cretaceous-Early Tertiary North-Central Montana alkalic province. Journal of Geophysical Research, v. 88, no. B12, p. 10,593-10,609.

Diller, J. S., 1902, Topographic Development of the Klamath Mountains. Bulletin of the United States Geological Survey No. 196. Washington, Department of the Interior, 63 p.

Dorf, E., 1930, Pliocene floras of California, Carnegie Institution of Washington Publication No. 412. Washington, Carnegie Institution of Washington, p. 1-108.

Dott, R. H. Jr., 1962, Geology of the Cape Blanco Area, Southwestern Oregon. ORE BIN, v. 24, no. 8, p. 121-133.

Dott, R. H. J., 1971, Geology of the Southwestern Oregon Coast West of the 124th Meridian. State of Oregon Department of Geology and Mineral Industries; Bulletin 69, 63 p.

Duque-Caro, H., 1990, Neogene stratigraphy, paleoceanography and paleobiogeography in northwest South America and the evolution of the Panama Seaway. Palaeogeography, Palaeoclimatology, Palaeoecology, v. 77, p. 203-234.

Durham, J. W., 1953, Miocene at Cape Blanco, Oregon. Geological Society of America Bulletin, abstracts v. 64, no. 12, pt. 2, p. 1504-1505.

Dziak, R. P., Fox, C. G., Bobbitt, A. M., and Goldfinger, C., 2001, Bathymetric Map of the Gorda Plate: Structural and Geomorphic Processes Inferred from Multibeam Surveys. Marine Geophysical Researches, v. 22, p. 235-250.

Emerson, L. F., and Retallack, G. J., 2005, A new middle Miocene flora from Cape Blanco, OR. Geological Society of America abstracts with programs, v. 37, no. 7, p. 362.

Emerson, L. F., and Retallack, G. J., 2007, Miocene coastal vegetation preserved by volcanic eruption at Cape Blanco, OR. Geological Society of America abstracts with programs, v. 39, no. 6, p. 401.

Erez, J., and Luz, B., 1983, Experimental paleotemperature equation for planktonic foraminifera. Geochimica et Cosmochimica Acta, v. 47, p. 1025-1031.

Ferguson, D. K., 1985, The Origin of Leaf-assemblages-New Light on an Old Problem. Review of Palaeobotany and Palynology, v. 46, p. 117-188.

Fields, P. F., 1996, The Succor Creek Flora of the middle Miocene Sucker Creek formation, southwestern Idaho and eastern Oregon; Systematics and Paleoecology [Dissertation thesis]. Michigan State University, 675 p.

Fisher, R., 1953, Dispersion on a Sphere. Proceedings of the Royal Society of London. Series A, Mathematical and Physical Sciences, v. 217, no. 1130, p. 295-305.

Forest, C. E., Wolfe, J. A., Molnar, P., and Emanuel, K. A., 1999, Paleoaltimetry incorporating atmospheric physics and botanical estimates of paleoclimate. Geologic Society of America Bulletin, v. 111, no. no. 4, p. 497-511.

Garver, J. I., and Scott, T. J., 1995, Trace elements in shale as indicators of crustal provenance and terrane accretion in the southern Canadian Cordillera. GSA Bulletin, v. 107, no. 4, p. 440-453.

Garzanti, E., Critelli, S., and Ingersoll, R. V., 1996, Paleogeographic and paleotectonic evolution of the Himalayan Range as reflected by detrital modes of Tertiary sandstones and modern sands (Indus transect, India and Pakistan). GSA Bulletin, v. 108, no. 6, p. 631-642.

Graham, A., 1963, Systematic Revision of the Sucker Creek and Trout Creek Miocene Floras of Southeastern Oregon. American Journal of Botany, v. 50, p. 921-936.

Greenwood, D. R., Wilf, P., Wing, S. L., and Christophel, D. C., 2004, Paleotemperature Estimation Using Leaf-Margin Analysis: Is Australia Different?. Palaios, v. 19, p. 129-142.

Gregory-Wodzicki, K. M., 2000, Relationships between leaf morphology and climate, Bolivia: implication for estimating paleoclimate from fossil floras. Paleobiology, v. 26, no. 4, p. 668-688.

Hammond, P. E., 1980, Reconnaissance Geologic Map and Cross Sections of Southern Washington Cascade Range. Department of Earth Sciences Portland State University, scale 1:125,000.

Haq, B. U., Hardenbol, J., and Vail, P. R., 1987, Chronology of Fluctuating Sea Levels since the Triassic. Science, v. 235, no. 4793, p. 1156-1167.

Harper, G. D., 1984, The Josephine ophiolite, northwestern California. Geological Society of America Bulletin, v. 95, p. 1009-1026.

Herold, N., Seton, M., Müller, R. D., You, Y., and Huber, M., 2008, Middle Miocene tectonic boundary conditions for use in climate models. Geochemistry Geophysics Geosystems, v. 9, no. 10, p. 1-10, doi:10.1029/2008GC002046.

Hickey, L. J., 1973, Classification of the Architecture of Dicotyledonous Leaves. American Journal of Botany, v. 60, no. 1, p. 17-33.

Hladky, F. R., 1994, Geologic Map of the Lakecreek Quadrangle, Jackson County, Oregon. Oregon Department of Geology and Mineral Industries Geological Map Series GMS-88, scale 1:24,000.

Hladky, F. R., 1996, Geology and Mineral Resources of Grizzly Peak Quadrangle, Jackson County, Oregon. State of Oregon Department of Geology and Mineral Industries Map Series-106, scale 1:24,000.

Hladky, F. R., 1999a, Geology and Mineral Resources Map of the Brownsboro Quadrangle, Jackson County, Oregon. State of Oregon Department of Geology and Mineral Industries Map Series-109, scale 1:24,000.

Hladky, F. R., 1999b, Geology and Mineral Resources of the Rio Canyon Quadrangle, Jackson County, Oregon, State of Oregon Department of Geology and Mineral Industries Map Series GMS-108, scale 1.24,000.

Hooghiemstra, H., and van der Hammen, T., 1998, Neogene and Quaternary development of the neotropical rainforest: the forest refugia hypothesis, and a literature overview. Earth-Science Reviews, v. 44, p. 147-183.

Hunt, R. M. Jr., and Stepleton, E., 2004, Geology and Paleontology of the Upper John Day Beds, John Day River Valley, Oregon: Lithostratigraphic and Biochronologic revision in the Haystack Valley and Kimberly Areas (Kimberly and Mt. Misery Quadrangles). Bulletin of the American Museum of Natural History, n. 282, p. 90.

Hunter, R. E., Clifton, H. E., and Phillips, R. L., 1979, Depositional processes, sedimentary structures, and predicted vertical sequences in barred nearshore systems, Southern Oregon Coast. Journal of Sedimentary Petrology, v. 49, no. 3, p. 711-726.

Janda, R. J., 1969, Age and correlation of marine terraces near Cape Blanco. Oregon, Geological Society of America meeting, Eugene, Oregon, abstract, p. 29-30.

Kelsey, H. M., 1990, Late Quaternary deformation of marine terraces on the Cascadia Subduction Zone near Cape Blanco, Oregon. Tectonics, v. 9, no. 5, p. 983-1014.

Kirschvink, J. L., 1980, The least-squares line and plane and the analysis of palaeomagnetic data. Geophysical Journal International, v. 62, p. 699-718.

Knowlton, F. H, 1898, A Report of the Fossil Plants of the Payette Formation, *in*, The Mining Districts of the Idaho Basin and the Boise Ridge, Idaho, by Waldemar Lindgren, *in,* Part Three of the 18th Annual Report of the United States Geological Survey. Washington, Department of the Interior, pages 721-735.

Knowlton, F. H., 1902, Fossil Flora of the John Day Basin Oregon. Washington, Government Printing Office, 150 p.

Knowlton, F. H., 1926, Flora of the Latah Formation of Spokane, Washington, and Coeur D' Alene, Idaho. Washington, Government Printing Office: Department of the Interior: Shorter contributions to general geology, 55 p.

Koch, J. G., 1966, Late Mesozoic stratigraphy and tectonic history, Port Orford-Gold Beach Area, Southwestern Oregon Coast. Bulletin of the American Association of Petroleum Geologists, v. 50, no. 1, p. 25-71.

Koppers, A. P., 2002, ArArCALC--software for $^{40}Ar/^{39}Ar$ age calculations. Computers & Geosciences, v. 28, p. 605-619.

Kuenzi, W. D., Horst, O. H., and McGehee, R. V., 1979, Effect of volcanic activity on fluvial-deltaic sedimentation in a modern arc-trench gap, southwestern Guatemala. Geological Society of America Bulletin, v. 90, p. 827-838.

Kürschner, W. M., Zvaček, Z., and Dilcher, D. L., 2008, The impact of Miocene atmospheric carbon dioxide fluctuations on climate and the evolution of terrestrial ecosystems. Proceedings of the National Academy of Sciences, v. 105, no. 2, p. 449-453.

Le Bas, M. J., Le Maitre, R. W., and Woolley, A. R., 1992, The Construction of the Total Alkali-Silica Chemical Classification of Volcanic Rocks. Mineralogy and Petrology, v. 46, p. 1-22.

Leithold, E. L., and Bourgeois, J., 1983, Sedimentology of the sandstone of Floras Lake (Miocene) transgressive, high-energy shelf deposition, SW Oregon, *in* Larue, D. K., and Steel, R. J., eds., Cenozoic Marine Sedimentation Pacific Margin, U.S.A.. Los Angeles, CA, The Pacific Section Society of Economic Paleontologist and Mineralogists, p. 17-28.

Lesquereux, L., 1878, Report of the Fossil Plants of the Auriferous Gravel Deposits of the Sierra Nevada. Memoirs of the Museum of Comparative zoology at Harvard College, v. 6, no. 2, p. 1-55.

Lesquereux, L., 1888, Recent determination of fossil plants from Kentucky, Louisiana, Oregon, California, Alaska, Greenland ect. with description of new species, *in* Clark, A. H., ed., Proceedings of the United States National Museum. Washington D.C., Government Printing Office, p. 11-38.

Lewis, J. C., Unruh, J. R., and Twiss, R. J., 2003, Seismogenic strain and motion of the Oregon coast block. Geology, v. 31, no. 2, p. 183-186.

MacGinitie, H.D., 1933, The Trout Creek Flora of Southeastern Oregon, Fossil Floras of Yellowstone National Park and Southeastern Oregon. Washington D.C., Carnegie Institution of Washington Publication No. 416, p.22-68

Magill, J., and Cox, A., 1980, Tectonic Rotation of the Oregon Western Cascades. Portland, Oregon, State of Oregon Department of Geology and Mineral Industries, 67 p.

Marincovich, L. J., and Gladenkov, A. Y., 1999, Evidence for an early opening of the Bering Strait. Nature, v. 397, p. 149-151.

McCaffrey, R., Long, M. D., Goldfinger, C., Zwick, P. C., Nabelek, J. L., Johnson, C. K., and Smith, C., 2000, Rotation and plate locking at the southern Cascadia subduction zone. Geophysical Research Letters, v. 27, no. 19, p. 3177-3120.

McDougall, I., and Harrison, T. M., 1999, Geochronology and Thermochronology by the $^{40}Ar/^{39}Ar$ Method. New York, Oxford University Press, 269 p.

Mertzman, S. A., 2000, K-Ar results from the southern Oregon-northern California Cascade Range. Oregon Geology, v. 62, no. 4, p. 99-122.

Meyer, H. W., and Manchester, S. R., 1997, The Oligocene Bridge Creek Flora of the John Day Formation, Oregon. Berkeley, University of California Press, 195 p.

Miller, I. M., Brandon, M. T., and Hickey, L. J., 2006, Using leaf margin analysis to estimate the mid-Cretaceous (Albian) paleolatitude of the Baja BC block. Earth and Planetary Science Letters, v. 245, p. 94-114.

Miller, M. M., Johnson, D. J., Rubin, C. M., Dragert, H., Wang, K., Qamar, A., and Goldfinger, C., 2001, GPS-determination of along-strike variation in Cascadia margin kinematics: Implications for relative plate motion, subduction zone coupling, and permanent deformation. Tectonics, v. 20, no. 2, p. 161-176.

Moore, E. J., 1963, Miocene Marine Mollusks from the Astoria Formation in Oregon, Geological Survey Professional Paper 419. Washington DC, United States Government Printing Office, 109 pages

Moore, E. J., and Addicott, W. O., 1987, The Miocene Pillarin and Newportian (Molluscan) Stages of Washington and Oregon and Their Usefulness in Correlations From Alaska to California, *in* Yochelson, E. L., ed., Shorter Contributions to Paleontology and Stratigraphy. Denver, CO, U. S. Geologic Survey, p. A1-A13.

Motoi, T., Chan, W.-L., Minobe, S., and Sumata, H., 2005, North Pacific halocline and cold climate induced by Panamanian gateway closure in a coupled ocean-atmosphere GCM. Geophysical Research Letters, v. 32, no. L10618, p. doi:10.1029/2005GL022844.

Murray, M. H., and Lisowski, M., 2000, Strain accumulation along the Cascadia subduction zone. Geophysical Research Letters, v. 27, no. 22, p. 3631-3634

Newberry, J. S., 1898, Later Extinct Floras of North America. Washington, Government Printing Office.

Niklas, K.J., Brown, R.M.J., Santos, R., and Vian, B., 1978, Ultrastructure and cytochimstry of Miocene angiosperm leaf tissues. Proceedings of the National Academy of Sciences, v. 75, p. 3263-3267.

Nikoleav, S. D., 1998, Neogene-Quaternary variations of the 'Pole-Equator' temperature gradient of the surface oceanic waters in the North Atlantic and North Pacific. Global and Planetary Change, v. 18, p. 85-111.

Ogg, J. G., and Smith, A. G., 2004, The geomagnetic polarity time scale, *in* Gradstein, F. M., Ogg, J. G., and Smith, A. G., eds., A Geologic Time Scale 2004. Cambridge, Cambridge University Press.

Oliver, E., 1936, A Miocene Flora from the Blue Mountains, Oregon, Middle Cenozoic Floras of Western North America. Washington D.C., Carnegie Institution of Washington: Publication No. 455, p. 1-27.

Opdyke, N. D., Lindsay, E. H., Johnson, N. M., and Downs, T., 1977, The Paleomagnetism and Magnetic Polarity Stratigraphy of the Mammal-Bearing Section of Anza Borrego State Park, California. Quaternary Research, v. 7, p. 316-329.

Orton, G. J., 1996, Volcanic environments, *in* Reading, H. G., ed., Sedimentary Environments: Processes, Facies and Stratigraphy. Oxford, Blackwell Sciences Ltd, p. 485-567.

Pluhar, C., Kirschvink, J.L., and Adams, R. W., 1991, Magnetostratigraphy and clockwise rotations of the Plio-Pleistocene Mojave River Formation, central Mojave desert, California. San Bernardino County Museum Association Quarterly, v., 38, p. 31-42.

Preist, G. R., Woller, N. M., and Black, G. L., 1983, Overview of the Geology of the Central Oregon Cascade Range, *in* Preist, G. R., and Vogt, B. F., eds., Geology and Geothermal Resources of the Central Cascade Range, Special Paper 15. Portland, OR, State of Oregon Department of Geology and Mineral Industries, p. 3-28.

Prothero, D. R., 2001, Chronostratigraphic calibration of the Pacific Coast Cenozoic: a summary, *in* Prothero, D. R., ed., Magnetic Stratigraphy of the Pacific Coast Cenozoic, Pacific Section SEPM Special Publication 91, p. 377-394.

Prothero, D. R., and Donohoo, L. L., 2001a, Magnetic stratigraphy and tectonic rotation of he lower Oligocene Tunnel Point Formation, Coos County, Oregon, *in* Prothero, D. R., ed., Magnetic Stratigraphy of the Pacific Coast Cenozoic, Pacific Section SEPM Special Publication 91, p. 195-200.

Prothero, D. R., and Donohoo, L. L., 2001b, Magnetic stratigraphy and tectonic rotation of the middle Eocene Coaledo Formation, southwestern Oregon. Geophysical Journal International, v. 145, p. 223-232.

Prothero, D. R., Lau, J. N., and Armentrout, J. M., 2001, Magnetic stratigraphy of the upper Miocene (Wishkahan) Empire Formation, Coos County, Oregon, *in* Prothero, D. R., ed., Magnetic Stratigraphy of the Pacific Coast Cenozoic, Pacific Section SEPM Special Publication 91, p. 284-292.

Reading, H. G., and Collinson, J. D., 1996, Clastic Coasts, *in* Reading, H. G., ed., Sedimentary Environments: Processes, Facies, and Stratigraphy. Oxford, Blackwell Sciences Ltd., p. 688.

Renne, P. R., Deino, A. L., Walter, R. C., Turrin, B. D., Swisher, C. C. III., Becker, T. A., Curtis, G. H., Sharp, W. D., and Jaouni, A.-R., 1994, Intercalibration of astronomical and radioisotopic time. Geology, v. 22, p. 783-786.

Renney, K. M., 1972, The Miocene Temblor Flora of West-Central California [Master of Science thesis]. University of California Davis, 106 p.

Retallack, G.J., 2004, Late Miocene climate and life on land in Oregon within a context of Neogene global change. Palaeogeography, Palaeoclimatology, Palaeoecology, v. 214, p. 97-123.

Retallack, G. J., 2007, Cenozoic Paleoclimate on Land in North America. The Journal of Geology, v. 115, p. 271-294.

Ruddiman, W. F. ed., 1997, Tectonic Uplift and Climate Change. New York, Plenum Press.

Sarna-Wojcicki, A. M., Lajoie, K. R., Meyer, C. E., and Adam, D. P., 1991, Tephrochronologic correlation of upper Neogene sediments along the Pacific margin, conterminous United States, *in* Morrison, R. B., ed., Quaternary nonglacial geology; Conterminous U. S.. Boulder, Colorado, Geological Society of America, p. 117-140.

Savage, J. C., Svarc, J. L., Prescott, W. H., and Murray, M. H., 2000, Deformation across the forearc of the Cascadia subduction zone at Cape Blanco, Oregon. Journal of Geophysical Research, v. 105, no. B2, p. 3095-3102.

Savin, S. M., Abel, L., Barrera, E., Hodell, D., Kennett, J. P., Murphy, M., Keller, G., Killingley, J., and Vincent, E., 1985, The evolution of Miocene surface and near-surface marine temperatures: Oxygen isotopic evidence, *in* Kennett, J. P., ed., The Miocene Ocean: Paleoceanography and Biogeography. Boulder, CO, The Geological Society of America, p. 49-82.

Schwerdtfeger, W., 1976, Climates of Central and South America. Amsterdam-Oxford-New York, Elsevier Scientific Publishing Company, p. 527.

Scott, K. M., 1988, Origins, Behavior, and Sedimentology of Lahars and Lahar-Runout Flows in the Toutle-Cowlitz River System, U.S. Geological Survey Professional Paper 1447-A. Washington, 74 p.

Selley, R. C., 2000, Applied Sedimentology. San Diego, Academic Press, 521 p.

Sewall, J. O., and Sloan, L. C., 2006, Come a bit closer: A high-resolution climate study of the early Paleogene Laramide foreland. Geology, v. 34, p. 81-84.

Sherrod, D. R., and Smith, J. G., 2000, Geologic Map of Upper Eocene to Holocene Volcanic and Related Rocks of the Cascade Range, Oregon. U.S. Geological Survey, scale 1:500,000.

Simpson, R. W., and Cox, A., 1977, Paleomagnetic evidence for tectonic rotation of the Oregon Coast Range. Geology, v. 5, p. 585-589.

Smith, G. A., 1988, Sedimentology of proximal to distal vocaniclastics dispersed across an active foldbelt: Ellensburg Formation (late Miocene), central Washington. Sedimentology, v. 35, p. 953-977.

Smith, H., 1932, The fossil flora of Rockville, OR [Masters thesis]. Eugene, University of Oregon.

Solomon, S., D. Qin, M. Manning, R.B. Alley, T. Berntsen, N.L. Bindoff, Z. Chen, A. Chidthaisong, J.M. Gregory, G.C. Hegerl, M. Heimann, B. Hewitson, B.J. Hoskins, F. Joos, J. Jouzel, V. Kattsov, U. Lohmann, T. Matsuno, M. Molina, N. Nicholls, J. Overpeck, G. Raga, V. Ramaswamy, J. Ren, M. Rusticucci, R. Somerville, T.F. Stocker, P. Whetton, R.A. Wood and D. Wratt, 2007: Technical Summary. In: *Climate Change 2007: The Physical Science Basis. Contribution of Working Group I to the Fourth Assessment Report of the Intergovernmental Panel on Climate Change* [Solomon, S., D. Qin, M. Manning, Z. Chen, M. Marquis, K.B. Averyt, M. Tignor and H.L. Miller (eds.)]. Cambridge University Press, Cambridge, United Kingdom and New York, NY, USA.

Swanson, D. A., 1989, Geologic maps of the French Butte and Greenhorn Buttes Quadrangles, Washington, Open-File Report 89-309, Department of the Interior, U.S. Geological Survey, 3 Sheets p.

Tanai, T., and Wolfe, J. A., 1977, Revisions of *Ulmus* and *Zelkova* in the middle and late Tertiary of western North America. Geological Survey Professional Paper 1026: Washington, United States Government Printing Office, 11 p.

Tucker, M. E., 2003, Sedimentary Rocks in the Field. West Sussex, John Wiley and Sons, 234 p.

USDA, NRCS. 2009. The PLANTS Database (http://plants.usda.gov, 6 April 2009). National Plant Data Center, Baton Rouge, LA 70874-4490 USA.

Verplanck, E. P., 1985, Temporal variations in volume and geochemistry of volcanism in the western Cascades, Oregon. [Ph.D. thesis] Oregon State University, 115 p.

Vessell, R. K., and Davies, D. K., 1981, Nonmarine sedimentation in an active fore arc basin. Society of Economic Paleontologist and Mineralogist Special Publication, No. 31, p. 31-45.

Warwick, P. D., Johnson, E. A., and Khan, I. H., 1998, Collision-induced tectonism along the northwestern margin of the Indian subcontinent as recorded in the Upper Paleocene to Middle Eocene strata of central Pakistan (Kirthar and Sulaiman Ranges). Palaeogeography, Palaeoclimatology, Palaeoecology, v. 142, p. 201-216.

Wells, R. E., 1990, Paleomagnetic Rotations and the Cenozoic Tectonics of the Cascade Arc, Washington, Oregon, and California. Journal of Geophysical Research, v. 95, no. B12, p. 19,409-19,417.

Wells, R. E., and Heller, P. L., 1988, The relative contribution of accretion, shear, and extension to Cenozoic tectonic rotation in the Pacific Northwest. Geological Society of America Bulletin, v. 100, p. 325-338.

Wells, R. E., and Simpson, R. W., 2001, Northward migration of the Cascadia forearc in the northwestern U.S. and implications for subduction deformation. Earth Planets Space, v. 53, p. 275-283.

Wells, R. E., Weaver, C. S., and Blakely, R. J., 1998, Fore-arc migration in Cascadia and its neotectonic significance. Geology, v. 26, no. 8, p. 759-762.

Wilf, P., 1997, When are Leaves Good Thermometers? A New Case for Leaf Margin Analysis. Paleobiology, v. 23, no. 3, p. 373-390.

Wilf, P., Wing, S. L., Greenwood, D. R., and Greenwood, C. L., 1998, Using fossil leaves as paleoprecipitaion indicators: An Eocene example. Geology, v. 26, no. 3, p. 203-206.

Wilson, D.S., 1989, Deformation of the so-called Gorda Plate. Journal of Geophysical Research, v. 94, p. 3065-3075.

Wing, S. L., Harrington, G. J., Smith, F. A., Bloch, J. I., Boyer, D. M., and Freeman, K. H., 2005, Transient Floral change and Rapid Global Warming at the Paleocene-Eocene Boundary. Science, v. 310, p. 993- 996.

Wing, S., L., and Greenwood, D. R., 1993, Fossils and Fossil Climate: The Case for Equable Continental Interiors in the Eocene. Philosophical Transactions- Royal Society of London. Biological Sciences, v. 341, no. 1297, p. 243-252.

Wolfe, J. A., 1964, Miocene Floras from Fingerrock Wash, southwestern Nevada. United States Geologic Survey Professional Paper 454-N: Washington, United States Government Printing Office, 36 p. 12 plates

Wolfe, J. A., 1966, Tertiary Plants from the Cook Inlet Region, Alaska. Geological Survey Professional Paper 398-B.

Wolfe, J. A., 1979, Temperature parameters of Humid to Mesic Forests of Eastern Asia and relation to forests of other regions of the Northern Hemisphere and Australasia, United States Geological Survey Professional Paper, 1106.

Wolfe, J.A., 1981, Paleoclimatic Significance of the Oligocene and Neogene Floras of the Northwestern United States, in Niklas, K.J., ed., Paleobotany, Paleoecology, and Evolution, Volume 2: New York, Praeger, p. 79-101.

Wolfe, J. A., 1993, A Method Of Obtaining Climatic Parameters From Leaf Assemblages, U. S. Geological Survey Bulletin 2040. Washington, United States Government Printing Office, 67 p.

Wolfe, J. A., 1994, Tertiary climatic changes at middle latitudes of western North America. Palaeogeography, Palaeoclimatology, Palaeoecology, v. 108, p. 195-205.

Wolfe, J. A., and Tanai, T., 1980, The Miocene Seldovia Point Flora from the Kenai Group, Alaska. United States Geological Survey Professional Paper 1105. Washington, United States Government Printing Office, 52 p. 25 plates.

Wolfe, J.A., and Tanai, T., 1987, Systematics, Phylogeny, and Distribution of Acer (Maples) in the Cenozoic of Western North America. Journal of the Faculty of Science, Hokkaido University, v. 22, p. 1-246.

Woodruff, F., and Savin, S. M., 1989, Miocene Deep Water Oceanography. Paleoceanography, v. 4, p. 87-140.

Zachos, J., Pagani, M., Sloan, L., Thomas, E., and Billups, K., 2001, Trends, Rhythms, and Aberrations in Global Climate 65 Ma to Present. Science, v. 292, p. 686-692.

Zachos, J., Stott, L. D., and Lohmann, K. C., 1994, Evolution of early Cenozoic marine temperatures. Paleoceanography, v. 9, no. 2, p. 353-387.